HHS Public Access

Author manuscript

*J Immunol*. Author manuscript; available in PMC 2019 April 01.

Published in final edited form as:

*J Immunol*. 2018 April 01; 200(7): 2426–2438. doi:10.4049/jimmunol.1700313.

# $\alpha_M\beta_2$ is anti-atherogenic in female but not male mice

**Dorota Szpak**[*], **Lahoucine Izem**[‡], **Dmitriy Verbovetskiy**[*], **Dmitry A. Soloviev**[*], **Valentin P. Yakubenko**[€], and **Elzbieta Pluskota**[*,#]

[*]Department of Molecular Cardiology, Cleveland Clinic, Cleveland, OH

[‡]Department of Molecular and Cellular Medicine, Cleveland Clinic, Cleveland, OH

[€]Department of Biomedical Sciences, Quillen College of Medicine, Johnson City, TN

## Abstract

Atherosclerosis is a complex inflammatory process characterized by monocyte recruitment into the arterial wall, their differentiation into macrophages and lipid accumulation. Since integrin $\alpha_M\beta_2$ (CD11b/CD18) mediates multiple diverse functions of leukocytes, we examined its role in atherogenesis.

$\alpha_M^{-/-}/ApoE^{-/-}$ and $ApoE^{-/-}$ mice were fed control or high fat diet (HFD) for 3 or 16 weeks to induce atherogenesis. Unexpectedly, $\alpha_M$ deficiency accelerated development of atherosclerosis in female but not in male mice. The size of aortic root lesions was 3–4.5-fold larger in female $\alpha_M^{-/-}/ApoE^{-/-}$ than in $ApoE^{-/-}$ mice. Monocyte/macrophage content within the lesions was increased 2.5-fold in female $\alpha_M^{-/-}/ApoE^{-/-}$ mice due to enhanced proliferation. $\alpha_M\beta_2$ elimination promoted gender-dependent foam cell formation due to enhanced uptake of cholesterol by $\alpha_M^{-/-}/ApoE^{-/--}$ macrophages. This difference was attributed to enhanced expression of lipid uptake receptors, CD36 and scavenger receptor A1 (SR-A1), in female mice. Macrophages from female $\alpha_M^{-/-}/ApoE^{-/-}$ mice showed dramatically reduced expression of FoxM1 transcription factor and estrogen receptors (ER) α and β. 17β-estradiol ($E_2$) decreased CD36, SR-A1 levels and foam cell formation in $ApoE^{-/-}$ macrophages in ERα– and ERβ-dependent manner, as their antagonists inhibited the effect of $E_2$. However, female $\alpha_M^{-/-}/ApoE^{-/-}$ macrophages failed to respond to $E_2$ and maintained elevated CD36, SR-A1 levels and lipid accumulation. FoxM1 inhibition in $ApoE^{-/-}$ macrophages reduced ERs and enhanced CD36, SR-A1 expression, while FoxM1 overexpression in $\alpha_M^{-/-}/ApoE^{-/-}$ macrophages reversed their proatherogenic phenotype.

We demonstrate a new, surprising atheroprotective role of $\alpha_M\beta_2$ in female $ApoE^{-/-}$ mice. $\alpha_M\beta_2$ maintains ER expression in macrophages and $E_2$-dependent inhibition of foam cell formation.

### Keywords

Atherosclerosis; Inflammation; Lipids and Cholesterol; Mechanisms; Aging; Women; Animal Models of Human Disease

[#]**To whom correspondence should be addressed:** Elzbieta Pluskota Ph.D., Department of Molecular Cardiology, Lerner Research Institute, Cleveland Clinic, 9500 Euclid Avenue, NB50, Cleveland, OH 44195, U.S.A., pluskote@ccf.org, Phone: (216) 455-8211, Fax: (216) 445-8204.

## Introduction

Atherosclerosis associated with hypercholesterolemia is a chronic inflammatory disease of the vessel wall, characterized by accumulation of cholesterol-loaded macrophages and fibrous material in lesions that develop in large arteries (1, 2). An initiating event is the accumulation of modified low-density lipoproteins (LDLs) in the vessel wall that cause endothelial dysfunction and trigger monocyte deposition in the sub-endothelial space. Transendothelial monocyte migration is a multistep process dependent upon several adhesion molecules including $\beta_1$ and $\beta_2$ integrins on leukocytes, which interact with intercellular adhesion molecule-1 (ICAM-1) and vascular cell adhesion molecule1 (VCAM-1) on endothelial cells (3, 4). Subsequently, monocytes differentiate into macrophages and uptake of oxidized LDLs (ox-LDLs) leads to formation of lipid-laden foam cells, the hallmark of atherosclerosis. Of the many scavenger receptors mediating the influx of lipids into the macrophages, the class A type I and II macrophage scavenger receptors (SR-AI and SR-AII) and CD36, are known to be centrally involved in foam cell formation (5–7). Later, these macrophages are further activated, resulting in the production of various inflammatory mediators including not only a wide range of cytokines and growth factors but also reactive oxygen species (ROS). These mediators stimulate recruitment and proliferation of additional immune cells and enhance lipid oxidation (1, 2).

The epidemiology of coronary heart disease shows that the incidence of deaths from heart attack in 35–64 year old men exceeds that in age-matched women by 500% (8). Consequently, multiple studies have focused on the potential role of female sex hormones, particularly estrogen, in prevention of atherosclerosis (reviewed in (9–12). Indeed, in mouse, rabbit and cynomolgus monkey models, estrogen has had anti-atherosclerotic effects when reintroduced early after ovariectomy (13–18). Estrogen fulfils this function by acting on virtually all types of cells implicated in atherogenesis. For example, it inhibits apoptosis, oxidative stress and expression of VCAM and ICAM-1 in endothelial cells as well as proliferation, migration, oxidation and release of inflammatory cytokines in smooth muscle cells (reviewed in (10)). In macrophages, short term treatment with estrogen not only decreases secretion of inflammatory cytokines but also reduces foam cell formation by inhibiting cholesterol accumulation (19–24). There are 3 estrogen receptors (ER): ERα, ERβ and G protein-coupled ER (GPR30). The majority of reports demonstrates that ERα exerts protective functions in animal models of atherosclerosis while the roles of ERβ and GPR30 are less well-defined (reviewed in (10)).

The $\beta_2$-integrins, $\alpha_L\beta_2$ (CD11a/CD18), $\alpha_M\beta_2$ (CD11b/CD18), $\alpha_X\beta_2$ (CD11c/CD18) and $\alpha_D\beta_2$ (CD11d/CD18), are involved in most leukocyte responses associated with atherosclerosis, including transendothelial extravasation, adhesion, phagocytosis and production of a variety of growth factors, cytokines and reactive oxygen species (ROS) (reviewed in (25)). Supporting the importance of the $\beta_2$ integrins in atherogenesis, $\beta_2$-deficient ($CD18^{-/-}$) mice fed a high fat diet (HFD) showed attenuated atherogenesis (4) and the $\alpha_X$- or $\alpha_M$-knockout mice in the $ApoE^{-/-}$ background showed reduced development of atherosclerotic lesions (26–27). The effect of the $\alpha_L$-deficiency on atherogenesis in any proatherogenic murine background ($ApoE^{-/-}$ or $LDLR^{-/-}$) has not been reported to date. Administration of an anti-$\alpha_M$ function blocking antibody to $LDLR^{-/-}$ mice with

hypercholesterolemia resulted in a 30% reduction in the size of atherosclerotic lesions as well as macrophage content within the plaques (28). Unexpectedly, bone marrow transplantation experiments from the $\alpha_M^{-/-}$ or WT mice into male $LDLR^{-/-}$ mice did not reveal any role to $\alpha_M\beta_2$ integrin in atherosclerosis (29). This inconsistency led us to further examine the role of $\alpha_M\beta_2$ in atherosclerosis. Using $\alpha_M^{-/-}/ApoE^{-/-}$ and $ApoE^{-/-}$ mice, we demonstrate a surprising, anti-atherogenic and gender-dependent role for $\alpha_M\beta_2$ in hyperlipidemic female $ApoE^{-/-}$ mice. Mechanistically, we find that $\alpha_M\beta_2$ exerts this gender-specific effect by supporting of macrophage ERα and ERβ expression and estrogen-dependent reduction of foam cell formation as a result of down-regulation of the lipid scavenger receptors CD36 and SR-A1.

## Materials and Methods

### Animals and Diet

The $\alpha_M$-deficient mice were described previously (30) and kindly provided by Dr. Christie Ballantyne (Baylor College of Medicine, Houston, TX). These mice were backcrossed to C57BL/6J background for 7 generations. $ApoE^{-/-}$ mice in C57BL/6J background were from Jackson Laboratories (Bar Harbor, ME) and crossbred with $\alpha_M^{-/-}$ mice to obtain littermate $\alpha_M^{-/-}/ApoE^{-/-}$ and $\alpha_M^{+/+}/ApoE^{-/-}$ mice (control mice designated as $ApoE^{-/-}$ mice throughout). Both male and female mice were used in the experiments. Atherosclerosis was induced by placing 4-week-old $\alpha_M^{-/-}/ApoE^{-/-}$ and $ApoE^{-/-}$ mice on a Western diet (High Fat Diet) containing 0.2% cholesterol and 42% calories as fat (TD88137, Harlan Teklad) for 3 or 16 weeks. Control chow diet contained 18% protein and 5% fat (Teklad Global 2918, Harlan Teklad). All procedures were performed under protocols approved by the Cleveland Clinic IACUC.

### Reagents and antibodies

Recombinant mouse GM-CSF and IL-4 were purchased from R&D Systems (Minneapolis, MN). The following antibodies were used for Western blot or FACS assays: mouse anti-CD36 (BD Biosciences, San Jose, CA), mouse anti-SRA-1 (R&D Systems), rabbit anti-SRB-1 (Thermoscientific), rat anti-LOX-1 and goat anti-CD206 (R&D Systems), rat anti-mouse ABCA-1 (Bio-Rad, Raleigh, NC), goat anti-ABCG-1and anti-Fox M1 (Santa Cruz, Dallas, TX), rabbit anti-PPARγ, rabbit anti-ERα, rabbit anti-ERβ (EMD Milipore, Temecula, CA) and mouse anti-β-actin and rabbit anti-iNOS (Cell Signaling Technology, Danvers, MA). Mouse FITC-conjugated anti-$\alpha_M$ mAb (clone M1/70), PE or FITC-conjugated F4/80 mAb, anti-$\alpha_L$-PE were from eBioscience (San Diego, CA). anti-$\alpha_X$-PE, anti-$\alpha_4$-PE mAbs were from (BD Biosciences, San Jose, CA). The anti-$\alpha_D$ antibody was provided by Dr. Yakubenko and was previously described (27). Low-density lipoprotein/very-low density lipoprotein (LDL/VLDL) cholesterol was measured in mouse plasma using an HDL & LDL/VLDL Cholesterol Quantification Kit. Triglyceride levels were analyzed using Triglyceride Quantification Colorimetric/Fluorometric Kit (BioVision Research Products, Milpitas, CA). 1,3-Bis(4-hydroxyphenyl)-4-methyl-5-[4-(2-piperidinylethoxy)phenol]-1H-pyrazole (MPP), an ERα antagonist, 4-[2-Phenyl-5,7-bis(trifluoromethyl)pyrazolo[1,5-α]pyrimidin-3-yl]phenol (PHTPP), a ERβ antagonist, were from Tocris Bioscience (Minneapolis, MN). Mouse IL-6, IL-12 p40/p70 and IL-10 Elisa kits

were from RayBiotech (Norcross, GA). All other reagents were purchased from Sigma-Aldrich (St. Louis, MO).

## Modified LDL preparation

LDL acetylation- LDL are combined with equal volume of saturated sodium acetate, mixed and cooled on ice. While continuously and slowly mixing the solution, the volume of the required acetic anhydride was added in 3 steps over 20 minute intervals. The modified LDL are then dialyzed overnight in the cold room against 100 fold excess of 09% NaCl, 0.05 EDTA, pH 7.4. The preparation is filtered through a 0.45 μm filter. The protein content is determined by Lowry method and the extent of lysine modification is determined using TNBS assay (2,4,6-trinitrobenzene sulfonic acid). The protein content of the acetylated LDL was >1mg/ml and the amount of modified lysine was ~58%. Each lot was >97% pure by agarose gel electrophoresis.

LDL oxidation-LDL was oxidized by incubating LDL with 5 μM CuSO4 in phosphate-buffered saline without EDTA for 20h at 37C. Oxidation was arrested by refrigeration and addition of 100 μM EDTA and 20 μM butylated hydroxytoluene. Control incubations were done without $CuS0_4$ and with EDTA and butylated hydroxytoluene added prior to incubation (31). Protein content was determined by Lowry assay and the degree of oxidation of LDL was tested by the measurement of LDL Thiobarbituric Acid-Reactive Substances (TBARS) in ox-LDL (32). Agarose gel electrophoresis analysis determined >98% purity of all preparations. Parallel experiments were performed using these modified lipoproteins purchased from Biomedical Technologies Inc. (Stoughton, MA).

## Lipid uptake assays

Cells were treated with serum containing RPMI medium supplemented with GM-CSF for 2 days, then incubated with medium containing 2% FBS and 50μg/ml of $^3$H-acetylated LDL for 2, 4, 6 or 12 hours. Upon removal of the medium, the cells were washed with cold PBS and harvested in 0.1N NaOH. Lipid uptake was determined by measuring the amount of radioactivity in the cells at different times. Proteins were determined by the Lowry method.

## Lipid efflux assays

Cells were treated with serum containing RPMI medium supplemented with GM-CSF for 2 days, then incubated with medium containing 2% FBS, 100μg/ml acetylated LDL and $^3$H-cholesterol (Perkin Elmer) for 24 hours. The medium was removed, the cells were washed 3 times with warm PBS and then incubated with RPMI containing 0.1% fatty acid free BSA and 100μg/ml human HDL for 6 hours. At the end of the efflux time, the medium was collected and the cells were washed 3 times with cold PBS and extracted in 0.1N NaOH. The radiolabel content of the cells was determined before the addition of the efflux medium and 12h after its addition.

## Atherosclerotic lesion analyses

Mice fed a HFD for 3 or 16 weeks were killed by ketamine/xylazine administration and perfused through the heart with PBS and 4% paraformaldehyde. For aortic sinus analysis, serial cryosections of 10-μm thickness were taken from the region of the proximal aorta

through the aortic sinus and stained with oil red O, hematoxylin and Light Green counterstain as described in (33). Although some red staining may be seen outside the aorta, only the oil red-O-filled lipid regions (lesions) on the luminal side of the internal elastic lamina covering the tunica media was measured using ImmagePro 7.0 software (see Supplemental Fig.1). For *en face* analysis, arch and descending aortas were removed, dissected free of fat, stained with oil red O followed by morphometry of scanned images using ImmagePro 7.0 software (Media Cybernetics, Bethesda, MD).

To analyze macrophage content and cell proliferation within aortic lesions, aortic root cryosections were stained with rat anti-mouse monocyte/macrophage Ab (MOMA-2) (EMD Millipore) or/and rabbit anti-Ki-67 Ab (Cell Signaling Technology) followed by secondary goat anti-rat or anti-rabbit IgG conjugated with Alexa568 or Alexa488 (Molecular Probes), respectively.

### *Ex vivo* foam cell formation

Thioglycollate-elicited peritoneal macrophages from 8–12 week-old $\alpha_M^{-/-}/ApoE^{-/-}$ and $ApoE^{-/-}$ mice fed a chow control diet were plated onto 8-well chamber slides (Lab-Tek) or 12-well plates (Corning) in DMEM F-12 medium. Non-adherent cells were removed after 2h and fresh medium containing 1% FBS and either native, ox-LDL or acetylated LDL (50 μg/ml) was added. The cells were incubated for 3 days. Cells in chamber slides were fixed with 4% formaldehyde, stained with oil red-O, counterstained with hematoxylin and mounted in VectaMount QS (Vector Laboratories) for microscopic analysis. Cells in 12-well plates were used to extract lipids and proteins as described (34, 35). Total cholesterol was quantified in lipid extracts using Cholesterol/Cholesteryl Quantification kit (Biovision, Milpitas, CA). Proteins were extracted from cells using 0.1M NaOH and measured by Bradford method (Biorad). Values of total cholesterol were normalized to total protein content of the extracts.

### *In vivo* foam cell formation

$\alpha_M^{-/-}/ApoE^{-/-}$ and $ApoE^{-/-}$ mice fed either HFD or control diets for 16 weeks were IP injected with thioglycollate and after 3 days, peritoneal cells were collected and plated in 8-well chamber slides or 12-well plates. Non-adherent cells were removed after 2 hours, and foam cells were evaluated by oil red-O staining or by measuring total cholesterol in cell extracts.

### Macrophage proliferation assay

The assays were performed as described (36, 37) with several modifications.

$ApoE^{-/-}$ and $\alpha_M^{-/-}/ApoE^{-/-}$ peritoneal macrophages were isolated 72 h after I.P. injection of 4% thioglycollate and plated at $2\times10^4$ cells/well in 96-well plates. After 2 hours, non-adherent cells were removed. Adherent macrophages were incubated in DMEM-F12 medium supplemented with 10% FBS in the presence of 50 μg/ml OxLDL or native LDL or 60ng/ml GM-CSF for 5 days. Proliferation was evaluated using CyQUANT® Direct Proliferation assay kit (Invitrogen Corporation, Carlsbad, CA). Briefly, medium was aspirated and the plates were frozen at −70°C for 2h. Plates were thawed and 150 μl of

freshly prepared Cyquant reagent were added per well. The plates were incubated for 15–30 min at room temperature, protected from light with gentle shaking and fluorescence at 480/530 nm was measured using Cytofluor II fluorometer (PerSeptive Biosystems, Framingham, MA). Calibration curve of fluorescence versus known numbers of macrophages was prepared. Number of adherent macrophages on day 0 was subtracted from the numbers of macrophages on day 5. Bone marrow was isolated from femur and tibia bones of $ApoE^{-/-}$ and $\alpha_M^{-/-}/ApoE^{-/-}$ mice. Macrophages were isolated from bone marrow suspensions using anti-F4/80 beads (Miltenyi Biotec, Auburn, CA) according to manufacturer's instructions. Proliferation assays were performed in the presence of 60ng/ml GM-CSF as described for peritoneal macrophages.

## FACS analysis of peritoneal macrophages

$ApoE^{-/-}$ and $\alpha_M^{-/-}/ApoE^{-/-}$ peritoneal cells were allowed to adhere to TC Petri dishes for 1 h, and adherent cells were recovered by brief trypsinization and preincubated with seroblock Ab (rat anti-mouse CD16/CD32) followed by incubation with Alexa488-labeled antibodies to SRA-1, CD36, ABCG1 and SRB-1 and PE-conjugated F4/80 Ab (eBioscience) for 30 min at 4°C. In polarization experiments, after incubation with LPS or IL-4 cells were briefly trypsinized, preincubated with seroblock Ab followed by incubation with Alexa488-labeled antibodies to iNOS or CD206 and PE-conjugated F4/80 Ab (eBioscience) for 30 min at 4°C. Cells were washed and analyzed in a FACSCalibur using CellQuest software (BD Biosciences, San Jose, CA). Isotype-matched control Abs were used as negative controls.

## Real-time qRT-PCR

Total RNA was extracted from peritoneal macrophages derived from $ApoE^{-/-}$ and $\alpha_M^{-/-}/ApoE^{-/-}$ mice fed HFD for 16 weeks using TRIzol reagent (Invitrogen), following the manufacturer's instructions. cDNA was generated using iScript™ cDNA Synthesis Kit (Bio-Rad, Berkeley, CA). qRT-PCR was performed using the respective gene-specific primers (SABiosciences, Valencia, CA) and the iQ™ SYBR Green Supermix on the Bio-Rad iCycler PCR system (Biorad) according to the manufacturer's instructions. The cycle threshold (Ct) values were calculated with SDS 1.4 software (Bio-Rad). The expression levels of each transcript were normalized using the $2^{-\Delta\Delta Ct}$ method (38) relative to GAPDH. The $\Delta C_t$ was calculated by subtracting the $C_t$ values of GAPDH from the $C_t$ values of the transcript of interest. The $\Delta\Delta C_t$ was then calculated by subtracting $\Delta C_t$ of the $ApoE^{-/-}$ macrophages from the $\Delta C_t$ of $\alpha_M^{-/-}/ApoE^{-/-}$ macrophages derived from mice of matching gender. Fold change in the gene was calculated according to the equation $2^{-\Delta\Delta Ct}$.

**Macrophage polarization experiments—**Equal numbers of resident peritoneal adherent macrophages ($2\times10^5$) from male and female $\alpha_M^{-/-}/ApoE^{-/-}$ and $ApoE^{-/-}$ mice were either untreated or stimulated with lipopolysaccharide LPS (1μg/ml) or mouse IL-4 (50 ng/ml) for 24–48 h to induce M1 or M2 polarization, respectively. After 24 h, cell conditioned media was collected and cells were subjected to Western blot with antibodies to iNOS and CD206. Alternatively, the cells were double stained for F4/80 and iNOS or CD206 and analyzed by FACS. The media were collected 48 h after stimulation and centrifuged at 5000×g for 10 min at 4°C, and IL-6, IL-12 (p40/p70) and IL-10 were assayed using specific ELISA kits (RayBiotech).

**Inhibition of $\alpha_M$ expression in *ApoE*$^{-/-}$ macrophages—**To reduce $\alpha_M$ expression, the *ApoE*$^{-/-}$ peritoneal macrophages of male and female mice were transfected with siGenome SMART pool mouse *Itgam* siRNAs or nontargeting (control) siRNA#2 (Thermo Scientific Dharmacon, Lafayette, CO) (100 nM) using GenMute siRNA transfection reagent (SignaGen Labs, Rockville, MD) according to manufacturer's instructions. After 48 h, macrophages were analyzed for capacity to form foam cells and by Western blot with antibodies to $\alpha_M$, Fox M1 ER-α and β, SR-A1, CD36 and β-actin.

**Modulation of Fox M1 expression in macrophages—**To reduce *Fox M1* expression, the *ApoE*$^{-/-}$ peritoneal macrophages of female mice were transfected with ON-TARGETplus SMART pool mouse *Fox M1* (small interfering RNA) siRNAs or ON-TARGETplus nontargeting pool siRNA (Thermo Scientific Dharmacon, Lafayette, CO) (100 nM) using GenMute siRNA transfection reagent. After 48 h, macrophages were subjected to Western blot with antibodies to $\alpha_M$, Fox M1, ER-α and β, SR-A1, CD36 and β-actin. To overexpress *Fox M1* in $\alpha_M^{-/-}$/*ApoE*$^{-/-}$ peritoneal macrophages isolated from female mice the mouse *Fox M1* cDNA was purchased from ABM Inc. (Vancouver, Canada) and recloned into pcDNA 3.1 vector using TOPO cloning kit. $2.5 \times 10^6$ macrophages were nucleofected with 2.5 μg of Fox M1-pcDNA 3.1 or empty pcDNA 3.1 vector using Mouse Macrophage Nucleofector Kit (Lonza, Allendale, NJ) and Y-001 program. Cells were seeded in ($2.5 \times 10^6$/well) in a 6-well plate in DMEM-F12 medium supplemented with 10% FBS and 10 ng/ml GM-CSF. After 5 days in culture, cells were subjected to Western blot and foam cell formation assays.

### Statistical analysis

Data are presented as means ± SEM. Statistical analyses were performed using Kolmogorov-Smirnov normality test followed by one-way ANOVA test and all pairwise multiple comparison tests with Holm-Sidak method (Sigma Plot 10.0 software, Systat Software Inc., San Jose, CA). A value of $P<0.05$ was considered significant.

## Results

### $\alpha_M\beta_2$ deficiency promotes atherosclerosis in female *ApoE*$^{-/-}$ mice

To study the role of $\alpha_M\beta_2$ in development of atherosclerosis, we subjected age- and gender-matched $\alpha_M^{-/-}$/*ApoE*$^{-/-}$ and *ApoE*$^{-/-}$ mice to chow or HFD for 3 or 16 weeks. Remarkably, atherosclerotic lesions were detected in the aortic roots in female $\alpha_M^{-/-}$/*ApoE*$^{-/-}$ mice as early as 3 weeks on HFD; their lesion areas were 3-fold larger than in female *ApoE*$^{-/-}$ ($P<0.001$, n=9) and male mice of both genotypes (Fig.1A). As atherosclerosis develops more slowly in mice fed chow diet rather than a HFD, after 16 weeks on chow diet the lesions were restricted to the aortic root. Under these conditions, a dramatic 4.5-fold increase in lesion area was observed in the $\alpha_M^{-/-}$/*ApoE*$^{-/-}$ female mice as compared to male $\alpha_M^{-/-}$/*ApoE*$^{-/-}$ and both genders of *ApoE*$^{-/-}$ mice ($P<0.001$, n=9). There was no significant difference in atherosclerotic lesion areas between male $\alpha_M^{-/-}$/*ApoE*$^{-/-}$ and *ApoE*$^{-/-}$ mice (Fig.1B, left panel). After 16 weeks on HFD, lesion areas in cross-sections of the aortic root were also increased by ~2-fold ($P<0.001$, n=9) in female $\alpha_M^{-/-}$/*ApoE*$^{-/-}$ mice compared to male $\alpha_M^{-/-}$/*ApoE*$^{-/-}$ and both genders of *ApoE*$^{-/-}$ mice (Fig.1C, left panel). Also, e*n face*

analyses of aortic arch and descending aorta at 16 weeks on HFD revealed a 2.5-fold increase in the aortic lesion area in female $\alpha_M^{-/-}/ApoE^{-/-}$ mice compared to their male counterparts and the $ApoE^{-/-}$ mice (P<0.001, n=9) (Fig.1D). Taken together, these data demonstrate that $\alpha_M\beta_2$ is protective against the initiation and progress of atherogenesis in a gender-specific manner.

## Increased monocyte/macrophage content in atherosclerotic lesions in the $\alpha_M^{-/-}/ApoE^{-/-}$ female mice

To begin to dissect the mechanism of enhanced lesion development in female $\alpha_M^{-/-}/ApoE^{-/-}$ mice, we examined macrophage/monocyte content in the lesions by staining cross-sections of the aortic roots with a monocyte/macrophage-specific mAb (MOMA-2). The macrophage content was increased by 2–2.5-fold (P<0.001, n=9) in female $\alpha_M^{-/-}/ApoE^{-/-}$ mice fed control or HF diet for 16 weeks as compared to all other groups tested (Fig.2 A and B). Macrophage content in the aortic root lesions was similar in male $\alpha_M^{-/-}/ApoE^{-/-}$ and both genders of the $ApoE^{-/-}$ mice on normal chow or HFD (Fig.2B). To examine macrophage proliferation in atherosclerotic lesions (39, 40), we double stained cross-sections of aortic roots of $\alpha_M^{-/-}/ApoE^{-/-}$ and $ApoE^{-/-}$ mice with MOMA-2 and an Ab to the Ki67 proliferation marker (Fig.2C and D). The Ki67-positive macrophages quantified as counts per MOMA-2-positive area were the most numerous (2–2.5-fold) in the lesions of the female $\alpha_M^{-/-}/ApoE^{-/-}$ compared to all other groups tested (P<0.001, n=9) (Fig.2D). Also, approximately 20–30% more macrophages proliferated in the lesions of male $\alpha_M^{-/-}/ApoE^{-/-}$ mice than of male $ApoE^{-/-}$ mice (P<0.05, n=9). However, there was no gender-dependent difference in macrophage proliferation in $ApoE^{-/-}$ mice (Fig.2D). These results were corroborated when we examined *ex vivo* proliferation of peritoneal macrophages isolated from $\alpha_M^{-/-}/ApoE^{-/-}$ and $ApoE^{-/-}$ mice fed control diet for 16 weeks (Fig.2E). GM-CSF and ox-LDL, but not native LDL, stimulated proliferation of macrophages isolated from all mouse lines. The $\alpha_M^{-/-}/ApoE^{-/-}$ macrophages showed enhanced proliferation as compared to the $ApoE^{-/-}$ macrophages. However, this difference was significantly more profound in female mice (~ 3-fold increase, P<0.001, n=6) than in male mice (~30–40% increase, P<0.05, n=6) (Fig.2E). Also, GM-CSF-induced proliferation of macrophages from bone marrow of female $\alpha_M^{-/-}/ApoE^{-/-}$ mice was increased by ~2-fold as compared to those from $ApoE^{-/-}$ mice, indicating that the difference in peritoneal macrophage proliferation is not tissue-specific (Supplemental Fig.1B). Thus, $\alpha_M\beta_2$ deficiency enhances macrophage/monocyte proliferation particularly in female mice. To examine macrophage apoptosis in atherosclerotic lesions, the cross-sections of aortic roots from $\alpha_M^{-/-}/ApoE^{-/-}$ and $ApoE^{-/-}$ mice were stained using a Tunel assay kit. Only a few apoptotic macrophages were detected in the lesions, and their numbers were similar in the $\alpha_M^{-/-}/ApoE^{-/-}$ and $ApoE^{-/-}$ mice (data not shown). Furthermore, when peritoneal $\alpha_M^{-/-}/ApoE^{-/-}$ and $ApoE^{-/-}$ macrophages were stained with Annexin V 24h after plating, no significant differences in the percent of early or late apoptotic cells between the mouse lines were found (data not shown).

In addition, we measured triglycerides, total cholesterol and VLDL/LDL cholesterol fraction in plasma of $\alpha_M^{-/-}/ApoE^{-/-}$ and $ApoE^{-/-}$ mice fed either HFD or chow diet for 16 weeks. The levels of these parameters were increased by 2–4-fold in mice on HFD; however, we did

not find any significant differences in these parameters between the $\alpha_M^{-/-}/ApoE^{-/-}$ and $ApoE^{-/-}$ mice or between genders (Supplemental Fig.2).

Also, we have compared expression levels of all members of the $\beta_2$-integrin subfamily and the $\alpha_4$ integrin on resident peritoneal macrophages derived from all mouse groups fed CD or HFD by FACS (Supplemental Table 1). First, expression levels of $\alpha_M$ integrin were similar in male and female $ApoE^{-/-}$ mice fed either control of HFD. Second, expression levels of the other β2-integrin members and α4 were not affected by the $\alpha_M$ deficiency or mouse gender as surface expression of $\alpha_L$, $\alpha_X$ and $\alpha_D$ and $\alpha_4$ was similar on macrophages derived $\alpha_M^{-/-}/ApoE^{-/-}$ and $ApoE^{-/-}$ mice of both genders. Third, crossing mice into $ApoE^{-/-}$ background did not change expression levels of the tested integrins and HFD diet did not affect expression of the $\beta_2$-integrins on the $ApoE^{-/-}$ macrophages of both genders. Although $\alpha_4$ expression was significantly decreased in mice fed HFD, its levels were the same in $\alpha_M^{-/-}/ApoE^{-/-}$ and $ApoE^{-/-}$ macrophages (Supplemental Table 1). Thus, the observed differences in monocyte/macrophage content in atherosclerotic lesions and atherogenic phenotype in female $\alpha_M^{-/-}/ApoE^{-/-}$ mice cannot be explained by altered levels of other integrin receptors on macrophages derived from these mice.

## $\alpha_M\beta_2$ deficiency supports pro-inflammatory M1 polarization of macrophages

The diverse functions of macrophages in immunity are reflected by several cellular phenotypes. A simplified scheme classifies macrophages as classically activated, pro-inflammatory (M1) and alternatively activated, anti-inflammatory (M2) (41). As progression of atherosclerotic lesions is correlated with the dominance of M1 macrophage polarization (42), we examined phenotypic polarization of $\alpha_M^{-/-}/ApoE^{-/-}$ and $ApoE^{-/-}$ peritoneal macrophages of male and female mice. Adherent macrophages were treated with LPS or IL-4 to induce M1or M2 polarization, respectively. The M1 markers: iNOS, IL-6 and IL-12(p40/p70) and M2 markers: CD206 and IL-10 were measured (Fig.3). Although iNOS was not detected by Western blot in untreated macrophages, FACS analysis showed a 2-fold increase in iNOS expression in the $\alpha_M^{-/-}/ApoE^{-/-}$ macrophages compared to $ApoE^{-/-}$ cells (Fig.3A and C). LPS stimulated iNOS expression by 2-fold in $ApoE^{-/-}$ cells and by 3–4-fold in $\alpha_M^{-/-}/ApoE^{-/-}$ macrophages. This led to a 3-fold and 6–8-fold enhancement of iNOS in male and female $\alpha_M^{-/-}/ApoE^{-/-}$ macrophages as compared to those from $ApoE^{-/-}$ mice (Fig.3A and C). Also, production of pro-inflammatory IL-6 and IL-12 was robustly augmented by 2.5–5-fold in $\alpha_M^{-/-}/ApoE^{-/-}$ cells compared to $ApoE^{-/-}$ macrophages regardless of LPS administration (Fig.3 E and F). In contrast, expression of CD206, the M2 marker, was significantly decreased in untreated macrophages from $\alpha_M^{-/-}/ApoE^{-/-}$ mice. IL-4 polarized $ApoE^{-/-}$ macrophages into the M2 phenotype and enhanced CD206 expression by 2-fold, but it failed to do so in $\alpha_M^{-/-}/ApoE^{-/-}$ macrophages (Fig.3B and D). Anti-inflammatory IL-10 production was decreased by 2–3-fold in resting cells and by-10–16-fold in IL-4-treated macrophages from $\alpha_M^{-/-}/ApoE^{-/-}$ mice, as these cells did not respond to IL-4 (Fig.3G). Taken together, the $\alpha_M^{-/-}/ApoE^{-/-}$ macrophages showed M1 polarization and were pro-inflammatory in gender-independent manner, although this feature was more profound in female mice.

### $\alpha_M\beta_2$ deficiency promotes foam cell formation

Accumulation of cholesterol in macrophages leading to foam cell formation is a crucial step in early atherogenesis. We examined whether $\alpha_M\beta_2$ affects foam cell formation *in vivo*. The $a_M^{-/-}/ApoE^{-/-}$ and $ApoE^{-/-}$ mice were fed HFD or control diet for 16 weeks; and an equal number of thioglycollate-elicited macrophages were evaluated for lipid and total cholesterol content. Regardless of genotype, macrophages harvested from mice on HFD showed increased oil red-O staining and total cholesterol content compared to those from mice fed chow diet (Fig.4A and B). However, regardless of the diet administered, intracellular lipid staining and total cholesterol content were increased by 2.5–4-fold in macrophages derived from female $a_M^{-/-}/ApoE^{-/-}$ mice compared to their male counterparts and $ApoE^{-/-}$ mice of both genders ($P<0.01$, n=8 mice) (Fig.4B). We also tested foam cell formation *ex vivo* by incubating thioglycollate-elicited macrophages from $a_M^{-/-}/ApoE^{-/-}$ and $ApoE^{-/-}$ female mice with native LDL, ox-LDL or acetylated LDL for 3 days. In contrast to native LDL, both ox-LDL and acetylated-LDL induced lipid accumulation in macrophages collected from both mouse lines. However, in the presence of modified LDLs, macrophages derived from the female $a_M^{-/-}/ApoE^{-/-}$ mice accumulated significantly more lipid and total cholesterol than cells isolated from male $a_M^{-/-}/ApoE^{-/-}$ animals and $ApoE^{-/-}$ mice of both genders (2–2.5-fold more, $P<0.001$, n=8 mice) (Fig.4C and D). To corroborate these data, we measured the kinetics of uptake of acetylated-LDL and efflux of $^3$H-cholesterol by and from the $a_M^{-/-}/ApoE^{-/--}$ and $ApoE^{-/-}$ peritoneal macrophages. At every time point, macrophages derived from female $a_M^{-/-}/ApoE^{-/-}$ mice showed a 2-fold increase in uptake of acetylated-LDL compared to their male littermates and $ApoE^{-/-}$ mice of both genders ($P<0.05$, n=5 mice) (Fig.4E). Also, the $a_M^{-/-}/ApoE^{-/-}$ macrophages had reduced lipid efflux (by ~30–40%, $P<0.01$, n=5 mice) compared to $ApoE^{-/-}$ cells and this difference was gender-independent (Fig.4F). Taken together, these results indicate that $\alpha_M\beta_2$ integrin suppresses foam cell formation by inhibiting macrophage lipid uptake and enhancing cholesterol efflux in female mice.

### Deletion of $\alpha_M\beta_2$ enhances expression of lipid uptake proteins and reduces expression of lipid efflux proteins

Knowing that $\alpha_M\beta_2$ regulates lipid uptake and efflux in macrophages, we examined expression levels of key proteins implicated in lipid metabolism. Peritoneal macrophages derived from $a_M^{-/-}/ApoE^{-/-}$ and $ApoE^{-/-}$ mice fed control diet or HFD for 16 weeks were analyzed by flow cytometry or Western blot using antibodies to the major scavenger receptors implicated in lipid uptake: CD36, SR-AI (scavenger receptor class A type I), proteins involved in cholesterol efflux such as transporter proteins: ABCA1 (ATP-binding cassette transporter), ATP-binding cassette sub-family G member 1 (ABCG1) and SR-B1(scavenger receptor class B type 1) (43, 44) as well as a nuclear receptor PPAR$\gamma$ (peroxisome proliferator-activated receptor $\gamma$), that regulates expression of most of these proteins which control lipid transport or metabolism (45). We did not find any differences in the expression of these proteins in the $a_M^{-/-}/ApoE^{-/-}$ and $ApoE^{-/-}$ macrophages derived from mice fed the control diet (Fig.5A–D) with the exception of PPAR$\gamma$, that was reduced in $a_M^{-/-}/ApoE^{-/-}$ macrophages. Interestingly, after the 16-week HFD, flow cytometry revealed a 3-fold- and 2-fold-increase ($P<0.01$, n=8 mice) in the expression of CD36 and SR-A1, respectively, on macrophages derived from $a_M^{-/-}/ApoE^{-/-}$ female mice compared to those

obtained from their male littermates and the *ApoE*$^{-/-}$ mice of both genders (Fig.5A, left panel). In contrast, expression levels of proteins mediating cholesterol efflux: ABCG1 and SR-B1 were dramatically reduced by ~60–70% on macrophages derived from $\alpha_M^{-/-}$/*ApoE*$^{-/-}$ mice than on those from *ApoE*$^{-/-}$ mice, but these differences were not gender-specific (Fig.5A, right panel). These data were corroborated by densitometric quantification of Western blot analyses of macrophage lysates (Fig.5B and C). CD36 and SR-A1 were dramatically enhanced in macrophages from $\alpha_M^{-/-}$/*ApoE*$^{-/-}$ female mice compared to those from male $\alpha_M^{-/-}$/*ApoE*$^{-/-}$ and *ApoE*$^{-/-}$ mice of both genders (Fig.5B and C). ABCG1, ABCA1 and SR-B1 levels were severely suppressed in $\alpha_M^{-/-}$/*ApoE*$^{-/-}$ macrophages compared to *ApoE*$^{-/-}$ cells but in gender-independent manner (Fig.5B and C). Also, PPARγ expression was extremely depressed in macrophages obtained from $\alpha_M^{-/-}$/*ApoE*$^{-/-}$ mice of both genders compared to those from *ApoE*$^{-/-}$ mice (Fig.5B and C). In general, expression levels of all tested proteins were elevated in macrophages of mice fed HFD as compared to control diet. HFD increased cholesterol efflux proteins: SR-B1, ABCG1, ABCA1 and PPARγ in *ApoE*$^{-/-}$ cells but not in $\alpha_M^{-/-}$/*ApoE*$^{-/-}$ macrophages. Also, HFD robustly augmented by 2–5-fold CD36 and SR-A1 expression in macrophages from female $\alpha_M^{-/-}$/*ApoE*$^{-/-}$ mice and no more than 2-fold in macrophages of all other mouse strains (Fig.5A–C).

Quantitative RT-PCR revealed a gender-specific enhancement of CD36 35-fold) and SR-A1 (5.5-fold) mRNA in macrophages from female $\alpha_M^{-/-}$/*ApoE*$^{-/-}$ mice fed HFD (Fig.5D, middle panel). In contrast, expression of SR-B1, ABCA-1, ABCG-1 and PPARγ transcripts was reduced by 50–80% in the $\alpha_M^{-/-}$/*ApoE*$^{-/-}$ macrophages, but in gender-independent manner (Fig.5C, right panel). Additionally, in mice fed control diet macrophage mRNA levels of these proteins were similar in all mouse strains except of PPARγ, that was decreased by 75% in $\alpha_M^{-/-}$/*ApoE*$^{-/-}$ macrophages in both genders. Numerous reports on mechanisms of atherogenesis show *ex vivo* experiments performed on TG-elicited peritoneal macrophages as they are the most similar to the macrophages in the inflammatory milieu of an atherosclerotic lesion (46–49). Since resident macrophages are expected to be less inflammatory, in control experiments we examined expression of these lipid modulators in resident peritoneal macrophages. Interestingly, densitometric analysis of Western blots and flow cytometry revealed similar expression patterns of these proteins on resident and TG-elicited peritoneal macrophages: gender-dependent enhancement of CD36 and SR-A1 and gender-independent reduction of PPARγ, ABCG1, ABCA1, SR-B1in $\alpha_M^{-/-}$/*ApoE*$^{-/-}$ macrophages (Supplemental Fig.3).

Taken together, $\alpha_M^{-/-}$/*ApoE*$^{-/-}$ macrophages from female mice, in addition to reduced expression of lipid efflux proteins, showed dramatic gender-specific increases of lipid uptake receptors CD36 and SR-A1 (at protein and mRNA levels), which ultimately led to enhanced foam cell formation.

## $\alpha_M\beta_2$ deficiency results in gender-dependent reduction in macrophage expression of estrogen receptors

To consider a potential mechanism for gender-dependence of enhanced atherosclerosis in female $\alpha_M^{-/-}$/*ApoE*$^{-/-}$ mice, we compared expression of the two major estrogen receptors,

α (ERα) and β (ERβ), in thioglycollate-elicited macrophages from $\alpha_M^{-/-}/ApoE^{-/-}$ and $ApoE^{-/-}$ mice. Densitometric quantification of Western blots of macrophage lysates revealed that both ERα and ERβ were dramatically (80–90%) reduced in macrophages derived from female $\alpha_M^{-/-}/ApoE^{-/-}$ mice as compared to their male littermates and the $ApoE^{-/-}$ mice of both genders (ERα:*P<0.05; ERβ:**P<0.01, n=6 mice/group) (Fig.6A and B). Also, mRNA levels of both ERs were decreased exclusively in macrophages isolated from female $\alpha_M^{-/-}/ApoE^{-/-}$ mice as compared to $ApoE^{-/-}$ mice: 50% reduced in mice fed control diet and 80–90% reduced in mice on HFD (P<0.001, n=8 mice/group) (Fig.6C). These results were confirmed by immunostaining for ERα and ERβ of aortic root sections from female $\alpha_M^{-/-}/ApoE^{-/-}$ and $ApoE^{-/-}$ mice fed HFD. The atherogenic lesions of $ApoE^{-/-}$ mice showed robust staining for both ERs: ERα- 90% and ERβ-75% of total lesion area (Fig.6D, left panel). In contrast, in the lesions of $\alpha_M^{-/-}/ApoE^{-/-}$ mice expression of both ERs was very low: ERα- 8% and ERβ-12% of total lesion area (Fig.6D, right panel).

## 17-β-estradiol ($E_2$) fails to reduce ox-LDL uptake as well as pro-inflammatory IL-6 and IL-12 secretion by macrophages derived from female $\alpha_M^{-/-}/ApoE^{-/-}$ mice

In view of multiple reports demonstrating inhibitory role of estrogen in foam cell formation (19–24), we measured the effect of $E_2$ on ox-LDL accumulation in macrophages isolated from $\alpha_M^{-/-}/ApoE^{-/-}$ and $ApoE^{-/-}$ mice of both genders. In the absence of $E_2$, ox-LDL uptake in macrophages was similar in male $\alpha_M^{-/-}/ApoE^{-/-}$ and in $ApoE^{-/-}$ mice of both genders, but it was augmented by 2-fold in female $\alpha_M^{-/-}/ApoE^{-/-}$ mice (Fig.7A and B). $E_2$ decreased lipid accumulation in macrophages of male $\alpha_M^{-/-}/ApoE^{-/-}$ and $ApoE^{-/-}$ mice by ~40% (P<0.01, n=6 mice), but failed to do so in those derived from female $\alpha_M^{-/-}/ApoE^{-/-}$ mice. In the presence of MPP or PHTPP, the antagonist of ERα and ERβ, respectively, the capacity of $E_2$ to reduce ox-LDL uptake by macrophages was inhibited by 50% when they were added separately and by 95–100% when they were added together, as compared to cells treated with $E_2$ alone. These results indicate that the inhibitory action of $E_2$ is driven by both ERs in macrophages from male $\alpha_M^{-/-}/ApoE^{-/-}$ and $ApoE^{-/-}$ mice. In contrast, not only $E_2$ but also neither of the ER antagonists showed any impact on foam cell formation from macrophages derived from female $\alpha_M^{-/-}/ApoE^{-/-}$ mice. This observation was consistent with the extremely low expression of both ERs in these cells (Fig.6A and B). Since CD36 and SR-A1 expression was significantly enhanced in macrophages obtained from female $\alpha_M^{-/-}/ApoE^{-/-}$ mice (Fig.5), we investigated the possibility that $E_2$ may regulate their expression via ERs. Densitometry of Western blots of macrophages derived from female $ApoE^{-/-}$ mice treated with ox-LDL and $E_2$ showed a 70% and 60% reduction in CD36 and SR-A1 immunostaining, respectively, as compared to cells not treated with $E_2$ (*P<0.05, n=6) (Fig.7C, right panel). MPP and PHTPP partially reversed the inhibitory effect of $E_2$ on CD36 and SR-A1 expression, while complete blockade of $E_2$ function was achieved by treating cells with both antagonists, implicating both ERα and ERβ in the response. Interestingly, like in the lipid uptake experiments, $E_2$ and ER antagonists did not affect CD36 and SR-A1 expression, which remained elevated in macrophages from female $\alpha_M^{-/-}/ApoE^{-/-}$ mice (Fig.7C). The changes in CD36 and SR-A1 protein levels were paralleled by changes in their mRNA levels. Specifically, CD36 and SR-A1 mRNA were attenuated by 50% in the presence of $E_2$ and both ER antagonists reversed $E_2$ effect in macrophages isolated from $ApoE^{-/-}$ female mice, while they had no effect on macrophages

derived from female $\alpha_M^{-/-}/ApoE^{-/-}$ mice (Fig.7D). In addition, $E_2$ attenuated secretion of IL-6 and IL-12 from macrophages derived from female $ApoE^{-/-}$ mice by ~50% and 70%, respectively (*P<0.05, n=6) through engagement of both ERs as their antagonists reduced the inhibitory effect of $E_2$. In contrast, $E_2$ and the ER antagonists failed to affect secretion of these inflammatory cytokines by macrophages from female $\alpha_M^{-/-}/ApoE^{-/-}$ mice, as they remained increased by 4–5-fold compared to $ApoE^{-/-}$ macrophages (Fig.7E).

**Fox M1 regulates expression of ERs in macrophages—**While nothing has been reported on the regulation of ER expression in macrophages, in breast cancer cells they are regulated by several Forkhead box (Fox) transcription factors including FoxO3, FoxA1 and Fox M1 (50–51). Densitometric analysis of Western blots revealed that HFD increased Fox M1 expression in macrophages from female $ApoE^{-/-}$ mice but not in female $\alpha_M^{-/-}/ApoE^{-/-}$ cells. Consequently, Fox M1 was reduced by ~70% in $\alpha_M^{-/-}/ApoE^{-/-}$ cells compared to $ApoE^{-/-}$ macrophages derived from female mice fed HFD (*P<0.05, n=6), while it was similar in macrophages from male mice of both mouse strains (Fig.8A and B). To elucidate if Fox M1 regulates ERs in macrophages we decreased its expression in peritoneal macrophages from $ApoE^{-/-}$ female mice fed HFD with siRNA. Densitometric analysis of Western blots showed that macrophage treatment with Fox M1 siRNA decreased Fox M1 expression by 85% as compared to untreated or control siRNA-treated macrophages (Fig.8C and D). Interestingly, the Fox M1reduction abrogated expression of both ERα and β by 90% and enhanced CD36 and SR-A1 levels by 2.5-fold indicating that it is an upstream regulator of these receptors in macrophages. In control Western blot, a decrease of Fox M1 did not affect $\alpha_M$ expression (Fig.8C and D). In addition, overexpression of Fox M1 in $\alpha_M^{-/-}/ApoE^{-/-}$ peritoneal macrophages from female mice enhanced expression of ERs and suppressed CD36 and SR-A1 expression as compared to untreated macrophages or transfected with the empty vector (Fig.8E). In the Fox M1 transfected $\alpha_M^{-/-}/ApoE^{-/-}$ macrophages, the levels of ERs and these scavenger receptors were similar to those observed in the $ApoE^{-/-}$ cells from female mice (Fig.8E). Consequently, with the attenuation of CD36 and SR-A1expression, the Fox M1- transfected $\alpha_M^{-/-}/ApoE^{-/-}$ macrophages showed a 2-fold reduction in foam cell formation by as compared to the control cells (Fig.8F). Taken together, we identify Fox M1 transcription factor as a key enhancer of ERs expression in macrophages and indirect (via ERs) regulator of CD36, SR-A1 levels and foam cell formation.

## Reduction of $\alpha_M$ expression in $ApoE^{-/-}$ macrophages decreases Fox M1 and FoxM1-dependent ER expression leading to enhanced foam cell formation in a gender-dependent manner

To elucidate if reduction of $\alpha_M$ expression in $ApoE^{-/-}$ macrophages would recapitulate the effects of the $\alpha_M$ deficiency observed in $\alpha_M^{-/-}/ApoE^{-/-}$ cells, we treated $ApoE^{-/-}$ macrophages derived from mice of both genders with nontargeting (control) and $\alpha_M$ specific siRNA. Densitometric analysis of the Western blots revealed that at 48h time point, this treatment reduced $\alpha_M$ expression by ~50% in macrophages derived from both male and female mice as compared to untreated cells or cells treated with nontargeting siRNA (Fig.9 A and B). Interestingly, this $\alpha_M$ attenuation, although only by 50%, led to a 70% reduction in FoxM1 expression and 50% and 70% inhibition of ERα and β expression, which was only observed in the $\alpha_M$ siRNA-treated $ApoE^{-/-}$ macrophages from female but not from

male mice. Also, while $\alpha_M$, FoxM1, ERα and β were decreased, the expression levels of SR-A1 and CD36 increased substantially in these cells (Fig.9A and B). Moreover, consistent with the enhanced CD36 and SR-A1 expression, foam cell formation also increased by 2.5-fold in $\alpha_M$ siRNA-treated $ApoE^{-/-}$ macrophages derived from female mice (Fig.9C) compared to untreated or control siRNA-treated macrophages. Taken together, the phenotype of $\alpha_M^{-/-}/ApoE^{-/-}$ female macrophages is similar to that of $ApoE^{-/-}$ female cells with a 50% $\alpha_M$ reduction. $\alpha_M$ siRNA-treatment inhibited FoxM1 expression only in female macrophages causing reduction of both ERs. Since ERs downregulate SR-A1 and CD36 (10, 19, 22), reduction of ERs likely led to increased expression of these scavenger receptors and enhanced foam cell formation.

## Discussion

We have demonstrated that integrin $\alpha_M\beta_2$ reduces atherogenesis in hypercholesterolemic female $ApoE^{-/-}$ mice. $\alpha_M\beta_2$ exerts this protective role via several mechanisms. First, it limits monocyte/macrophage accumulation within developing atherosclerotic lesions. Second, it suppresses classical M1 proinflammatory polarization in macrophages. Third, this integrin restricts foam cell formation by modulating levels of cholesterol transport proteins. The latter function is achieved by maintaining (via FoxM1 transcription factor) sufficient expression of ERα and ERβ in macrophages and their responses to $E_2$, which downregulates cholesterol uptake proteins CD36 and SRA-1.

These findings are quite unexpected in view of several previous reports showing reduced atherogenesis in mice deficient in the adhesion molecules that mediate leukocyte transendothelial extravasation, including ICAM-1, VCAM-1or P-selectin (3, 4) or $\alpha_X\beta_2$ (26). However, reports on the role of $\alpha_M\beta_2$ in atherosclerosis have been contradictory. Bone marrow adoptive transfer from $\alpha_M^{-/-}$ mice to male $LDLR^{-/-}$ mice concluded that $\alpha_M\beta_2$ is not involved in atherosclerosis (29). In contrast, inhibition of the integrin with specific blocking antibodies in $LDLR^{-/-}$ mice resulted in reduced development of atherosclerosis which was attributed to neutralization of the CD40 Ligand binding function of $\alpha_M\beta_2$ (28). However, mouse atherosclerosis models performed in the $ApoE^{-/-}$ versus $LDLR^{-/-}$ backgrounds do sometimes yield contradictory results (52). $\alpha_M\beta_2$ expression is increased on the surface of peripheral blood leukocytes of patients with ischemic heart disease indicative of their activated state (53), and it becomes severely down-regulated on macrophages derived from rabbit atherosclerotic lesions or in skin blisters of patients with stable coronary artery disease (54, 55). These reports are consistent with our data and suggest that deficiency or reduction of $\alpha_M$ expression could enhance atherosclerosis in humans.

The atherosclerotic lesions in the $\alpha_M^{-/-}/ApoE^{-/-}$ mice contained more macrophages than those in the $ApoE^{-/-}$ mice. This difference might be caused either by enhanced monocyte recruitment or by attenuated macrophage egress from the lesions. The latter possibility seems more likely in view of the data by Cao et al. (56) demonstrating defective emigration of $\alpha_M^{-/-}$ macrophages from the sites of inflammation into lymph nodes. Also, enhanced transendothelial migration into the vessel wall seems rather unlikely. Although the $\alpha_M^{-/-}/ApoE^{-/-}$ macrophages are still able to use other $\beta_2$-integrins or $\beta_1$-integrins ($\alpha_4\beta_1$ or $\alpha_5\beta_1$) for this function, we did not observe enhanced expression of any of these integrins to

compensate for the lack of $\alpha_M\beta_2$ (Supplemental Table 1). Furthermore, $\alpha_M^{-/-}$ leukocytes do not show impaired migration into the peritoneal cavity (30). Many studies demonstrated the capacity of macrophages to proliferate within atherosclerotic lesions (39), and apoptosis is also a pivotal process regulating macrophage numbers in lesions (40). Our data, however, suggests that $\alpha_M\beta_2$ plays a negligible role in macrophage survival, and the proatherogenic phenotype of the $\alpha_M^{-/-}/ApoE^{-/-}$ mice appears to be independent of apoptosis as we saw no difference in the Tunnel reactivity in lesions of male and female $\alpha_M^{-/-}/ApoE^{-/-}$ mice. Interestingly, the $\alpha_M^{-/-}/ApoE^{-/-}$ macrophages showed augmented proliferation in response to ox-LDL or GM-CSF *ex vivo* and in the atherosclerotic plaques in female mice. Our results are consistent with other studies demonstrating that murine peritoneal macrophages can proliferate in response to ox-LDL or GM-CSF *ex vivo* (36, 37). The effect of female sex hormones on macrophage proliferation has not been previously reported.

We have also demonstrated that $\alpha_M\beta_2$ elimination enhances proinflammatory, classical M1polarization of resident peritoneal macrophages at baseline and in response to LPS. The $\alpha_M^{-/-}/ApoE^{-/-}$ macrophages show a robust increase in the levels of proinflammatory markers, iNOS, IL-6 and IL-12, potentially leading to acceleration or enhancement of atherogenesis. Although these features were also observed in male mice, they are more pronounced in female mice. These data are consistent with Khallou-Laschet et al. who demonstrated that progression of atherosclerotic lesions is correlated with the domination of M1 over M2 macrophage polarization (41, 42) and with the reports of impaired M2 polarization in the $\alpha_M$-deficient macrophages (57).

Our data clearly demonstrate that $\alpha_M\beta_2$ deficiency leads to a significant female-dependent enhancement of foam cell formation. This enhancement is caused by an increase in modified lipids uptake which is attributable to augmented expression of two pivotal scavenger receptors, CD36 and SR-AI, in the $\alpha_M^{-/-}/ApoE^{-/-}$ macrophages of female mice, but not of male mice. In seeking a mechanism underlying this gender dependent effect, we determined that macrophages of female $\alpha_M^{-/-}/ApoE^{-/-}$ mice express extremely low levels of two estrogen receptors, ERα and ERβ; both the mRNA and protein expression levels of ERα and ERβ were suppressed in female $\alpha_M^{-/-}/ApoE^{-/-}$ mice. Furthermore, macrophage treatment with $E_2$ reduced CD36 and SR-A1 expression as well as cholesterol uptake by $ApoE^{-/-}$ macrophages, but not by female $\alpha_M^{-/-}/ApoE^{-/-}$ cells. The $E_2$-induced response of $ApoE^{-/-}$ macrophages was dependent on both ERs as MPP and PHTPP, antagonists of ERα and ERβ, respectively, reversed the effect of $E_2$. Thus, the absence of response to $E_2$ in $\alpha_M^{-/-}/ApoE^{-/-}$ macrophages is likely due to insufficient expression of ERs. This interpretation is consistent with multiple reports demonstrating atheroprotective role of estrogens and their receptors. First, myeloid–specific ERα deficiency accelerates atherosclerosis development in female mice (20) and ERβ engagement with a selective agonist decreases atherosclerotic lesions via secretion of atheroprotective heat shock protein (HSP27) in female $ApoE^{-/-}$ mice (22, 58, 59). Second, in cynomolgus macaques, rabbit and mouse models, $E_2$ supplementation ameliorated atherosclerosis under hypercholesterolemic conditions when started soon after ovariectomy (13–18). Third, the best characterized anti-atherogenic effect of estrogens on macrophages is female-specific suppression of foam cell formation. Estrogen via ERα decreases uptake of modified LDLs by reducing or inhibiting expression of cholesterol uptake proteins, CD36 and SR-A1 (19, 22, 21, 60); and by increasing

expression of several proteins, ABCA-1, ApoE and SR-B1 (20, 23, 24, 61, 62), that mediate cholesterol efflux. Thus, elevation of CD36 and SR-A1 expression in macrophages of $\alpha_M^{-/-}/ApoE^{-/-}$ mice is consistent with the loss of inhibitory action of $E_2$ due to attenuated ERs. We also noted reduced cholesterol efflux in the $\alpha_M^{-/-}/ApoE^{-/-}$ macrophages likely caused by decreased expression of ABCA-1, ABCG-1 and scavenger receptor SR-B1, in both female and male mice. However, we do not exclude that ABCA-1, ABCG-1 and SR-B1 reduction also contributes to enhanced foam cell formation in $\alpha_M^{-/-}/ApoE^{-/-}$ macrophages in female mice.

Thus, we have shown that a major mechanism of $\alpha_M\beta_2$–dependent, female-specific atheroprotection arises from its role as a regulator of ERs expression in macrophages to support all estrogen-mediated responses of these cells. This is the first report implicating integrins in regulation of expression of nuclear receptors such as ERs. For the first time, we also demonstrate that FoxM1 transcription factor enhances expression of both ERs in macrophages and that $\alpha_M\beta_2$ supports FoxM1 expression in gender-dependent-fashion. The latter interpretation is based on the observation that siRNA-induced decrease of $\alpha_M$ expression caused FoxM 1 reduction exclusively in macrophages derived from female, but not from male $ApoE^{-/-}$ mice. Importantly, FoxM1 expression in $\alpha_M^{-/-}/ApoE^{-/-}$ macrophages reverses the pro-atherogenic phenotype by elevating ERs, decreasing CD36, SR-A1 and foam cell formation. However, we cannot exclude other potential mechanisms or involvement of other Fox transcription factors. For example, $\alpha_M\beta_2$ enhances expression of c-fms proto-oncogene through reduction of FoxP1 (Forkhead box P1) transcription factor (63, 64) and c-fms is crucial to estrogen-induced increase of ERα and β expression (65). In addition, other questions can now be considered. For example, which other estrogen-mediated responses are altered in $\alpha_M^{-/-}/ApoE^{-/-}$ macrophages, are other leukocyte subsets in female $\alpha_M^{-/-}/ApoE^{-/-}$ mice affected in similar way or whether integrin $\alpha_M\beta_2$ limits macrophage proliferation and whether this effect depends on ERs.

The benefits of hormone replacement therapy in postmenopausal women in prevention and therapy of cardiovascular diseases remains controversial, but the outcome of hormonal therapy does seem to be better when commenced early during pre-menopause (12, 17, 66–68). Our work confirms atheroprotective advantages of estrogen replacement therapy. Finally, our results suggest that macrophage-targeted activation of $\alpha_M\beta_2$ might represent a novel strategy to limit early atherosclerosis in women at risk for cardiovascular diseases.

## Supplementary Material

Refer to Web version on PubMed Central for supplementary material.

## Acknowledgments

**Sources of funding**

This work was supported by funding from NIAID (AIO 80596 to D.A.S.) American Heart Association Scientist Development Grant 0335088N to E.P. Support for these studies were also provided by NIH grants from the Heart, Lung and Blood Institute (R01 HL17964, P01 HL076491 and P01 HL07331 to Edward F. Plow).

## Non-standard abbreviations

| | |
|---|---|
| **SR-A1** | scavenger receptor class A type I |
| **SR-B1** | scavenger receptor class B type 1 |
| **ABCA1** | ATP-binding cassette transporter A1 |
| **ABCG1** | ATP-binding cassette sub-family G member 1 |
| **PPARγ** | peroxisome proliferator-activated receptor γ |
| **HFD** | high fat diet |
| **ERα** | estrogen receptor alpha |
| **ERβ** | estrogen receptor beta |
| **LPS** | lipopolysaccharide |
| **CD** | control diet |
| **HFD** | high fat diet |

## References


1. Glass CK, Witztum JL. Atherosclerosis. the road ahead. Cell. 2001; 104:503–516. [PubMed: 11239408]
2. Libby P, Hansson GK. Inflammation and immunity in diseases of the arterial tree: players and layers. Circ. Res. 2015; 116:307–311. [PubMed: 25593275]
3. Bourdillon MC, Poston RN, Covacho C, Chignier E, Bricca G, McGregor JL. ICAM-1 deficiency reduces atherosclerotic lesions in double-knockout mice (ApoE(−/−)/ICAM-1(−/−)) fed a fat or a chow diet. Arterioscler. Thromb. Vasc. Biol. 2000; 20:2630–2635. [PubMed: 11116064]
4. Nageh MF, Sandberg ET, Marotti KR, Lin AH, Melchior EP, Bullard DC, Beaudet AL. Deficiency of inflammatory cell adhesion molecules protects against atherosclerosis in mice. Arterioscler. Thromb. Vasc. Biol. 1997; 17:1517–1520. [PubMed: 9301629]
5. Podrez EA, Febbraio M, Sheibani N, Schmitt D, Silverstein RL, Hajjar DP, Cohen PA, Frazier WA, Hoff HF, Hazen SL. Macrophage scavenger receptor CD36 is the major receptor for LDL modified by monocyte-generated reactive nitrogen species. J. Clin. Invest. 2000; 105:1095–1108. [PubMed: 10772654]
6. Febbraio M, Podrez EA, Smith JD, Hajjar DP, Hazen SL, Hoff HF, Sharma K, Silverstein RL. Targeted disruption of the class B scavenger receptor CD36 protects against atherosclerotic lesion development in mice. J. Clin. Invest. 2000; 105:1049–1056. [PubMed: 10772649]
7. Boullier A, Bird DA, Chang MK, Dennis EA, Friedman P, Gillotre-Taylor K, Horkko S, Palinski W, Quehenberger O, Shaw P, Steinberg D, Terpstra V, Witztum JL. Scavenger receptors, oxidized LDL, and atherosclerosis. Ann. N. Y. Acad. Sci. 2001; 947:214–222. [PubMed: 11795269]
8. Tunstall-Pedoe H, Kuulasmaa K, Amouyel P, Arveiler D, Rajakangas AM, Pajak A. Myocardial infarction and coronary deaths in the World Health Organization MONICA Project. Registration procedures, event rates, and case-fatality rates in 38 populations from 21 countries in four continents. Circulation. 1994; 90:583–612. [PubMed: 8026046]
9. Resanovic I, Rizzo M, Zafirovic S, Bjelogrlic P, Perovic M, Savic K, Patti AM, Isenovic RE. Anti-atherogenic effects of 17 beta-estradiol. Horm. Metab Res. 2013; 45:701–708. [PubMed: 23681753]
10. Nofer JR. Estrogens and atherosclerosis: insights from animal models and cell systems. J. Mol. Endocrinol. 2012; 48:R13–R29. [PubMed: 22355098]

11. Ng MK, Jessup W, Celermajer DS. Sex-related differences in the regulation of macrophage cholesterol metabolism. Curr. Opin. Lipidol. 2001; 12:505–510. [PubMed: 11561169]
12. Villablanca AC, Jayachandran M, Banka C. Atherosclerosis and sex hormones: current concepts. Clin. Sci. (Lond). 2010; 119:493–513. [PubMed: 20958265]
13. Hodgin JB, Krege JH, Reddick RL, Korach KS, Smithies O, Maeda N. Estrogen receptor alpha is a major mediator of 17 beta-estradiol's atheroprotective effects on lesion size in Apoe−/− mice. J. Clin. Invest. 2001; 107:333–340. [PubMed: 11160157]
14. Elhage R, Arnal JF, Pieraggi MT, Duverger N, Fievet C, Faye JC, Bayard F. 17 beta-estradiol prevents fatty streak formation in apolipoprotein E-deficient mice. Arterioscler. Thromb. Vasc. Biol. 1997; 17:2679–2684. [PubMed: 9409242]
15. Sophonsritsuk A, Appt SE, Clarkson TB, Shively CA, Espeland MA, Register TC. Differential effects of estradiol on carotid artery inflammation when administered early versus late after surgical menopause. Menopause. 2013; 20:540–547. [PubMed: 23615645]
16. Choi BG, Vilahur G, Zafar MU, Cardoso L, Yadegar D, Ibanez B, Tunstead J, Viles-Gonzalez JF, Schaffler MB, Fuster V, Badimon JJ. Selective estrogen receptor modulation influences atherosclerotic plaque composition in a rabbit menopause model. Atherosclerosis. 2008; 201:76–84. [PubMed: 18367192]
17. Cann JA, Register TC, Adams MR, St Clair RW, Espeland MA, Williams JK. Timing of estrogen replacement influences atherosclerosis progression and plaque leukocyte populations in ApoE−/− mice. Atherosclerosis. 2008; 201:43–52. [PubMed: 18374339]
18. Mayer LP, Dyer CA, Eastgard RL, Hoyer PB, Banka CL. Atherosclerotic lesion development in a novel ovary-intact mouse model of perimenopause. Arterioscler. Thromb. Vasc. Biol. 2005; 25:1910–1916. [PubMed: 15994440]
19. McCrohon JA, Nakhla S, Jessup W, Stanley KK, Celermajer DS. Estrogen and progesterone reduce lipid accumulation in human monocyte-derived macrophages: a sex-specific effect. Circulation. 1999; 100:2319–2325. [PubMed: 10587335]
20. Ribas V, Drew BG, Le JA, Soleymani T, Daraei P, Sitz D, Mohammad L, Henstridge DC, Febbraio MA, Hewitt SC, Korach KS, Bensinger SJ, Hevener AL. Myeloid-specific estrogen receptor alpha deficiency impairs metabolic homeostasis and accelerates atherosclerotic lesion development. Proc. Natl. Acad. Sci. U. S. A. 2011; 108:16457–16462. [PubMed: 21900603]
21. Allred KF, Smart EJ, Wilson ME. Estrogen receptor-alpha mediates gender differences in atherosclerosis induced by HIV protease inhibitors. J. Biol. Chem. 2006; 281:1419–1425. [PubMed: 16299001]
22. Rayner K, Chen YX, McNulty M, Simard T, Zhao X, Wells DJ, de BJ, O'Brien ER. Extracellular release of the atheroprotective heat shock protein 27 is mediated by estrogen and competitively inhibits acLDL binding to scavenger receptor-A. Circ. Res. 2008; 103:133–141. [PubMed: 18566345]
23. Liu M, Zhang W, Li X, Han J, Chen Y, Duan Y. Impact of age and sex on the development of atherosclerosis and expression of the related genes in apoE deficient mice. Biochem. Biophys. Res. Commun. 2016; 469:456–462. [PubMed: 26592663]
24. Dong P, Xie T, Zhou X, Hu W, Chen Y, Duan Y, Li X, Han J. Induction of macrophage scavenger receptor type BI expression by tamoxifen and 4-hydroxytamoxifen. Atherosclerosis. 2011; 218:435–442. [PubMed: 21820658]
25. Tan SM. The leucocyte beta2 (CD18) integrins: the structure, functional regulation and signalling properties. Biosci. Rep. 2012; 32:241–269. [PubMed: 22458844]
26. Wu H, Gower RM, Wang H, Perrard XY, Ma R, Bullard DC, Burns AR, Paul A, Smith CW, Simon SI, Ballantyne CM. Functional role of CD11c+ monocytes in atherogenesis associated with hypercholesterolemia. Circulation. 2009; 119:2708–2717. [PubMed: 19433759]
27. Aziz MH, Cui K, Das M, Brown KE, Ardell CL, Febbraio M, Pluskota E, Han J, Wu H, Ballantyne CM, Smith JD, Cathcart MK, Yakubenko VP. The Upregulation of Integrin alphaDbeta2 (CD11d/CD18) on Inflammatory Macrophages Promotes Macrophage Retention in Vascular Lesions and Development of Atherosclerosis. J. Immunol. 2017; 198:4855–4867. [PubMed: 28500072]
28. Zirlik A, Maier C, Gerdes N, MacFarlane L, Soosairajah J, Bavendiek U, Ahrens I, Ernst S, Bassler N, Missiou A, Patko Z, Aikawa M, Schonbeck U, Bode C, Libby P, Peter K. CD40 ligand

mediates inflammation independently of CD40 by interaction with Mac-1. Circulation. 2007; 115:1571–1580. [PubMed: 17372166]

29. Kubo N, Boisvert WA, Ballantyne CM, Curtiss LK. Leukocyte CD11b expression is not essential for the development of atherosclerosis in mice. J. Lipid Res. 2000; 41:1060–1066. [PubMed: 10884286]
30. Lu H, Smith CW, Perrard J, Bullard D, Tang L, Entman ML, Beaudet AL, Ballantyne CM. LFA-1 is sufficient in mediating neutrophil emigration in Mac-1 deficient mice. J. Clin. Invest. 1997; 99:1340–1350. [PubMed: 9077544]
31. Steinbrecher UP. Oxidation of human low density lipoprotein results in derivatization of lysine residues of apolipoprotein B by lipid peroxide decomposition products. J. Biol. Chem. 1987; 262:3603–3608. [PubMed: 3102491]
32. Yokode M, Kita T, Kikawa Y, Ogorochi T, Narumiya S, Kawai C. Stimulated arachidonate metabolism during foam cell transformation of mouse peritoneal macrophages with oxidized low density lipoprotein. J. Clin. Invest. 1988; 81:720–729. [PubMed: 3125226]
33. Baglione J, Smith JD. Quantitative assay for mouse atherosclerosis in the aortic root. Methods Mol. Med. 2006; 129:83–95. [PubMed: 17085806]
34. Das R, Ganapathy S, Mahabeleshwar GH, Drumm C, Febbraio M, Jain M, Plow EF. Macrophage Gene Expression and Foam Cell Formation is Regulated by Plasminogen. Circulation. 2013; 127:1209–1218. [PubMed: 23401155]
35. Robinet P, Wang Z, Hazen SL, Smith JD. A simple and sensitive enzymatic method for cholesterol quantification in macrophages and foam cells. J. Lipid Res. 2010; 51:3364–3369. [PubMed: 20688754]
36. Senokuchi T, Matsumura T, Sakai M, Yano M, Taguchi T, Matsuo T, Sonoda K, Kukidome D, Imoto K, Nishikawa T, Kim-Mitsuyama S, Takuwa Y, Araki E. Statins suppress oxidized low density lipoprotein-induced macrophage proliferation by inactivation of the small G protein-p38 MAPK pathway. J. Biol. Chem. 2005; 280:6627–6633. [PubMed: 15611087]
37. Lamharzi N, Renard CB, Kramer F, Pennathur S, Heinecke JW, Chait A, Bornfeldt KE. Hyperlipidemia in concert with hyperglycemia stimulates the proliferation of macrophages in atherosclerotic lesions: potential role of glucose-oxidized LDL. Diabetes. 2004; 53:3217–3225. [PubMed: 15561953]
38. Schmittgen TD, Livak KJ. Analyzing real-time PCR data by the comparative C(T) method. Nat. Protoc. 2008; 3:1101–1108. [PubMed: 18546601]
39. Robbins CS, Hilgendorf I, Weber GF, Theurl I, Iwamoto Y, Figueiredo JL, Gorbatov R, Sukhova GK, Gerhardt LM, Smyth D, Zavitz CC, Shikatani EA, Parsons M, Van RN, Lin HY, Husain M, Libby P, Nahrendorf M, Weissleder R, Swirski FK. Local proliferation dominates lesional macrophage accumulation in atherosclerosis. Nat. Med. 2013; 19:1166–1172. [PubMed: 23933982]
40. Andres V, Pello OM, Silvestre-Roig C. Macrophage proliferation and apoptosis in atherosclerosis. Curr. Opin. Lipidol. 2012; 23:429–438. [PubMed: 22964992]
41. Tugal D, Liao X, Jain MK. Transcriptional control of macrophage polarization. Arterioscler. Thromb. Vasc. Biol. 2013; 33:1135–1144. [PubMed: 23640482]
42. Khallou-Laschet J, Varthaman A, Fornasa G, Compain C, Gaston AT, Clement M, Dussiot M, Levillain O, Graff-Dubois S, Nicoletti A, Caligiuri G. Macrophage plasticity in experimental atherosclerosis. PLoS. One. 2010; 5:e8852. [PubMed: 20111605]
43. Westerterp M, Bochem AE, Yvan-Charvet L, Murphy AJ, Wang N, Tall AR. ATP-binding cassette transporters, atherosclerosis, and inflammation. Circ. Res. 2014; 114:157–170. [PubMed: 24385509]
44. Phillips MC. Molecular mechanisms of cellular cholesterol efflux. J. Biol. Chem. 2014; 289:24020–24029. [PubMed: 25074931]
45. Rigamonti E, Chinetti-Gbaguidi G, Staels B. Regulation of macrophage functions by PPAR-alpha, PPAR-gamma, and LXRs in mice and men. Arterioscler. Thromb. Vasc. Biol. 2008; 28:1050–1059. [PubMed: 18323516]
46. Li AC, Binder CJ, Gutierrez A, Brown KK, Plotkin CR, Pattison JW, Valledor AF, Davis RA, Willson TM, Witztum JL, Palinski W, Glass CK. Differential inhibition of macrophage foam-cell

formation and atherosclerosis in mice by PPARalpha, beta/delta, and gamma. J. Clin. Invest. 2004; 114:1564–1576. [PubMed: 15578089]

47. Yvan-Charvet L, Pagler TA, Seimon TA, Thorp E, Welch CL, Witztum JL, Tabas I, Tall AR. ABCA1 and ABCG1 protect against oxidative stress-induced macrophage apoptosis during efferocytosis. Circ. Res. 2010; 106:1861–1869. [PubMed: 20431058]
48. Tsimikas S, Miyanohara A, Hartvigsen K, Merki E, Shaw PX, Chou MY, Pattison J, Torzewski M, Sollors J, Friedmann T, Lai NC, Hammond HK, Getz GS, Reardon CA, Li AC, Banka CL, Witztum JL. Human oxidation-specific antibodies reduce foam cell formation and atherosclerosis progression. J. Am. Coll. Cardiol. 2011; 58:1715–1727. [PubMed: 21982317]
49. Huo Y, Zhao L, Hyman MC, Shashkin P, Harry BL, Burcin T, Forlow SB, Stark MA, Smith DF, Clarke S, Srinivasan S, Hedrick CC, Pratico D, Witztum JL, Nadler JL, Funk CD, Ley K. Critical role of macrophage 12/15-lipoxygenase for atherosclerosis in apolipoprotein E-deficient mice. Circulation. 2004; 110:2024–2031. [PubMed: 15451785]
50. Madureira PA, Varshochi R, Constantinidou D, Francis RE, Coombes RC, Yao KM, Lam EW. The Forkhead box M1 protein regulates the transcription of the estrogen receptor alpha in breast cancer cells. J. Biol. Chem. 2006; 281:25167–25176. [PubMed: 16809346]
51. Giamas G, Filipovic A, Jacob J, Messier W, Zhang H, Yang D, Zhang W, Shifa BA, Photiou A, Tralau-Stewart C, Castellano L, Green AR, Coombes RC, Ellis IO, Ali S, Lenz HJ, Stebbing J. Kinome screening for regulators of the estrogen receptor identifies LMTK3 as a new therapeutic target in breast cancer. Nat. Med. 2011; 17:715–719. [PubMed: 21602804]
52. Zampolli A, Bysted A, Leth T, Mortensen A, De CR, Falk E. Contrasting effect of fish oil supplementation on the development of atherosclerosis in murine models. Atherosclerosis. 2006; 184:78–85. [PubMed: 15946668]
53. Kassirer M, Zeltser D, Prochorov V, Schoenman G, Frimerman A, Keren G, Shapira I, Miller H, Roth A, Arber N, Eldor A, Berliner S. Increased expression of the CD11b/CD18 antigen on the surface of peripheral white blood cells in patients with ischemic heart disease: further evidence for smoldering inflammation in patients with atherosclerosis. Am. Heart J. 1999; 138:555–559. [PubMed: 10467208]
54. Gray JL, Shankar R. Down regulation of CD11b and CD18 expression in atherosclerotic lesion-derived macrophages. Am. Surg. 1995; 61:674–679. [PubMed: 7618805]
55. Paulsson JM, Dadfar E, Held C, Jacobson SH, Lundahl J. In vivo transmigrated monocytes from patients with stable coronary artery disease have a reduced expression of CD11b. Clin. Exp. Immunol. 2008; 153:196–204. [PubMed: 18460014]
56. Cao C, Lawrence DA, Strickland DK, Zhang L. A specific role of integrin Mac-1 in accelerated macrophage efflux to the lymphatics. Blood. 2005; 106:3234–3241. [PubMed: 16002427]
57. Jawhara S, Pluskota E, Cao W, Plow EF, Soloviev DA. Distinct Effects of Integrins alphaXbeta2 and alphaMbeta2 on Leukocyte Subpopulations during Inflammation and Antimicrobial Responses. Infect. Immun. 2017; 85:e00644–61. [PubMed: 27799334]
58. Rayner K, Sun J, Chen YX, McNulty M, Simard T, Zhao X, Wells DJ, de BJ, O'Brien ER. Heat shock protein 27 protects against atherogenesis via an estrogen-dependent mechanism: role of selective estrogen receptor beta modulation. Arterioscler. Thromb. Vasc. Biol. 2009; 29:1751–1756. [PubMed: 19729610]
59. Sun J, Ma X, Chen YX, Rayner K, Hibbert B, McNulty M, Dhaliwal B, Simard T, Ramirez D, O'Brien E. Attenuation of atherogenesis via the anti-inflammatory effects of the selective estrogen receptor beta modulator 8beta-VE2. J. Cardiovasc. Pharmacol. 2011; 58:399–405. [PubMed: 21697723]
60. Wilson ME, Sengoku T, Allred KF. Estrogen prevents cholesteryl ester accumulation in macrophages induced by the HIV protease inhibitor ritonavir. J. Cell Biochem. 2008; 103:1598–1606. [PubMed: 17879945]
61. Liang X, He M, Chen T, Wu Y, Tian Y, Zhao Y, Shen Y, Liu Y, Yuan Z. 17 beta-estradiol suppresses the macrophage foam cell formation associated with SOCS3. Horm. Metab Res. 2013; 45:423–429. [PubMed: 23430591]
62. Billon-Gales A, Fontaine C, Douin-Echinard V, Delpy L, Berges H, Calippe B, Lenfant F, Laurell H, Guery JC, Gourdy P, Arnal JF. Endothelial estrogen receptor-alpha plays a crucial role in the

atheroprotective action of 17 beta-estradiol in low-density lipoprotein receptor-deficient mice. Circulation. 2009; 120:2567–2576. [PubMed: 19996016]

63. Shi C, Zhang X, Chen Z, Sulaiman K, Feinberg MW, Ballantyne CM, Jain MK, Simon DI. Integrin engagement regulates monocyte differentiation through the forkhead transcription factor Foxp1. J. Clin. Invest. 2004; 114:408–418. [PubMed: 15286807]
64. Shi C, Sakuma M, Mooroka T, Liscoe A, Gao H, Croce KJ, Sharma A, Kaplan D, Greaves DR, Wang Y, Simon DI. Down-regulation of the forkhead transcription factor Foxp1 is required for monocyte differentiation and macrophage function. Blood. 2008; 112:4699–4711. [PubMed: 18799727]
65. Galal N, El-Beialy WR, Deyama Y, Yoshimura Y, Suzuki K, Totsuka Y. Novel effect of estrogen on RANK and c-fms expression in RAW 264.7 cells. Int. J. Mol. Med. 2007; 20:97–101. [PubMed: 17549395]
66. Meyer MR, Haas E, Barton M. Need for research on estrogen receptor function: importance for postmenopausal hormone therapy and atherosclerosis. Gend. Med. 2008; 5(Suppl A):S19–S33. [PubMed: 18395680]
67. Stygar D, Masironi B, Eriksson H, Sahlin L. Studies on estrogen receptor (ER) alpha and beta responses on gene regulation in peripheral blood leukocytes in vivo using selective ER agonists. J. Endocrinol. 2007; 194:101–119. [PubMed: 17592025]
68. Ostan R, Monti D, Gueresi P, Bussolotto M, Franceschi C, Baggio G. Gender, aging and longevity in humans: an update of an intriguing/neglected scenario paving the way to a gender-specific medicine. Clin. Sci. (Lond). 2016; 130:1711–1725. [PubMed: 27555614]

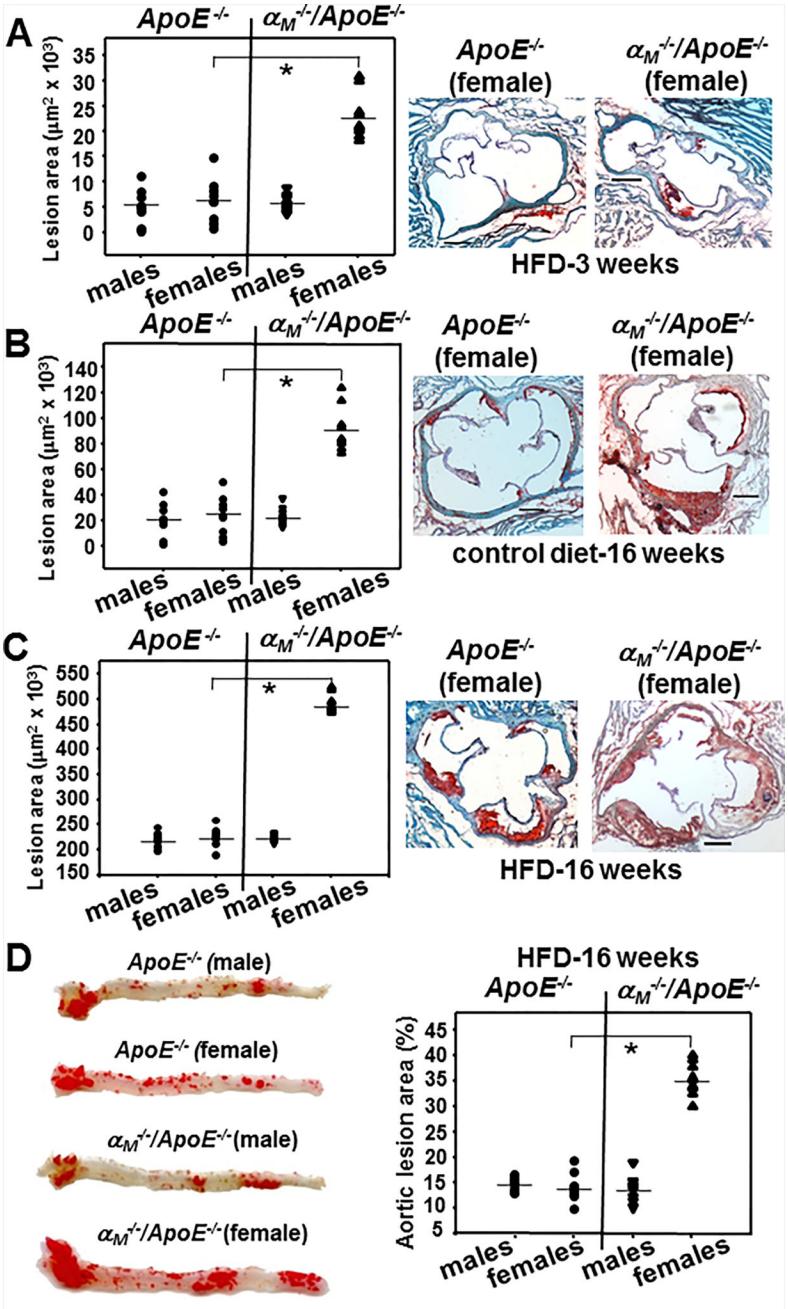


**Figure 1. Integrin $\alpha_M\beta_2$ deficiency enhances atherosclerosis in female *ApoE*$^{-/-}$ mice**

(A–C) (Right panels). Representative images of oil red O stained cross-sections of aortic roots of female $\alpha_M^{-/-}/ApoE^{-/-}$ and $ApoE^{-/-}$ mice fed HFD for 3 weeks (A), control chow diet (B), or HFD (C) for 16 weeks. Bar size, 122 μm (Left panels) Lesion area in oil red O-stained aortic roots was quantified as described in Methods. (*P<0.001, n=9 mice/group). (D) (Left panel) Representative images of *en face* oil red O staining of aortas of $\alpha_M^{-/-}/ApoE^{-/-}$ and $ApoE^{-/-}$ mice fed HFD for 16 weeks. (Right panel) Quantification of atheromatous area (*P<0.001, n=9 mice/group). The data are representative of 3 independent experiments.

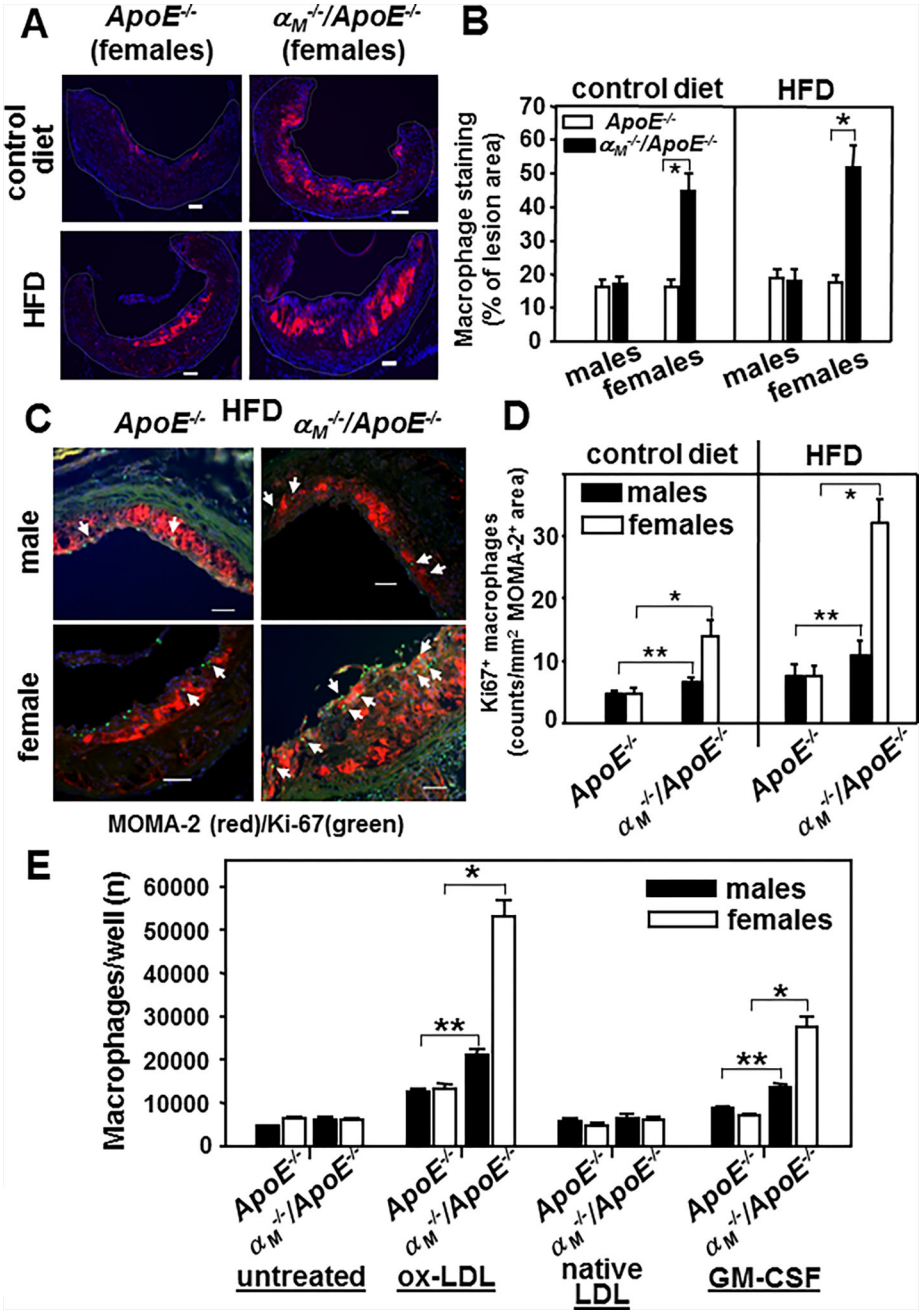


**Figure 2. Macrophages are increased in atherosclerotic lesions of female $\alpha_M^{-/-}/ApoE^{-/-}$ mice due to enhanced proliferation**

(A) Representative images of the aortic root sections stained with anti-monocyte/macrophage mAb (MOMA-2) (red). Female $\alpha_M^{-/-}/ApoE^{-/-}$ and $ApoE^{-/-}$ mice were fed chow or HFD for 16 weeks. Bar size, 64 μm (B) Quantification of MOMA-$2^+$ area in aortic roots of female and male $\alpha_M^{-/-}/ApoE^{-/-}$ and $ApoE^{-/-}$ mice. Data are expressed as % of lesion area. For each value, an average from at least 4 sections was calculated. (*P<0.001, female $\alpha_M^{-/-}/ApoE^{-/-}$ *vs* female $ApoE^{-/-}$ mice, n=9 mice) (C) Representative images of aortic roots of $\alpha_M^{-/-}/ApoE^{-/-}$ and $ApoE^{-/-}$ mice (fed HFD for 16 weeks) double-stained with Ab to Ki67 proliferation marker (green) and the monocyte/macrophage-specific

MOMA-2 (red). Bar size, 64 μm (D) Quantification of proliferating macrophages as $Ki67^{+}$ counts per MOMA-$2^{+}$ area. (*P<0.001, female $\alpha_M^{-/-}/ApoE^{-/-}$ *vs* female $ApoE^{-/-}$ mice; **P<0.05, male $\alpha_M^{-/-}/ApoE^{-/-}$ *vs* male $ApoE^{-/-}$ mice n=9 mice) (E) Proliferation of peritoneal macrophages isolated from the $\alpha_M^{-/-}/ApoE^{-/-}$ and $ApoE^{-/-}$ mice fed control diet for 16 weeks. Macrophages were cultured in the presence of native or ox-LDL (50μg/ml) or GM-CSF (60 ng/ml) for 5 days. The cell numbers at time 0 were subtracted. (*P<0.001, female $\alpha_M^{-/-}/ApoE^{-/-}$ *vs* female $ApoE^{-/-}$ mice and **P<0.05, male $\alpha_M^{-/-}/ApoE^{-/-}$ *vs* male $ApoE^{-/-}$ mice, n=8 mice). Data are representative of four independent experiments.

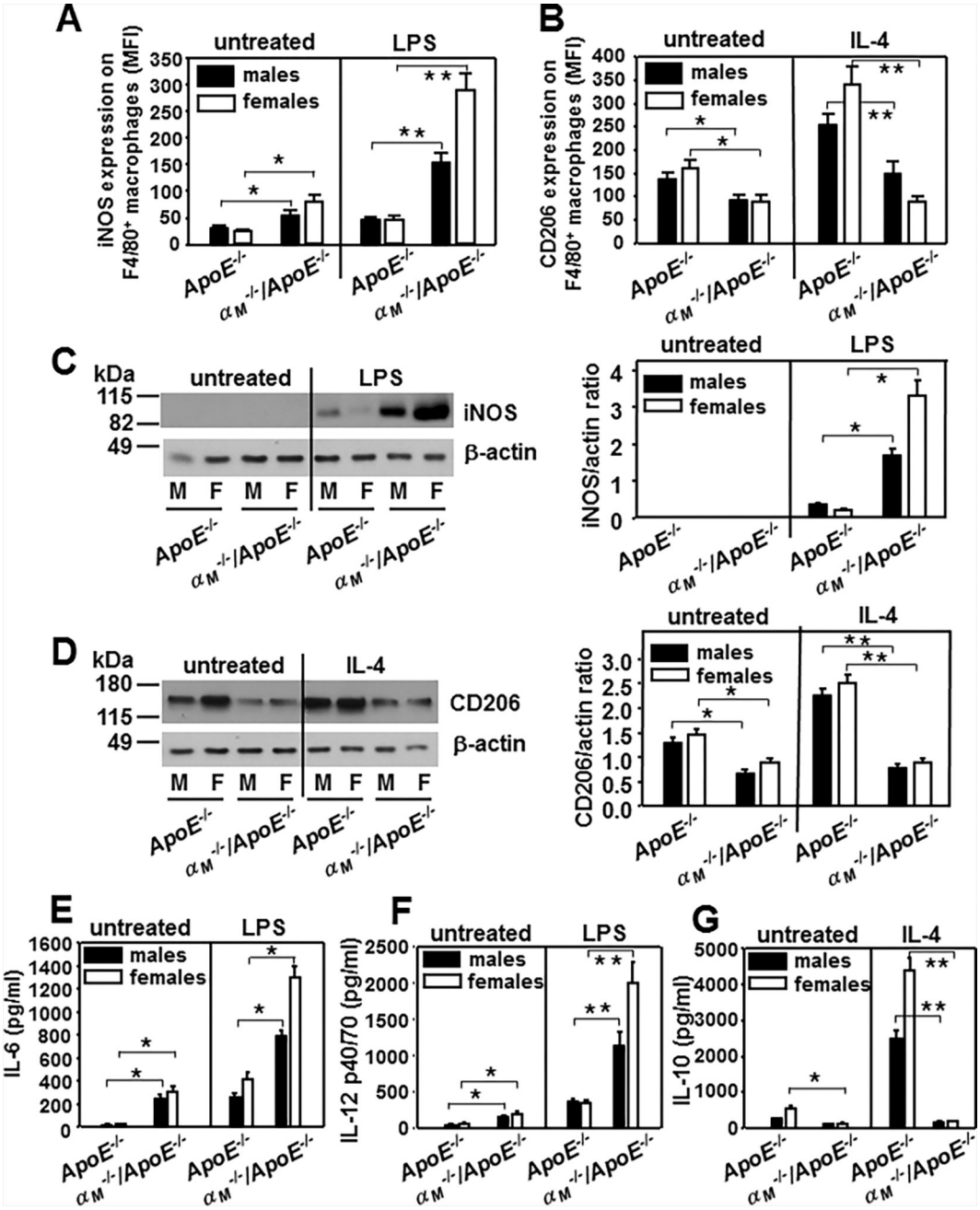


**Figure 3. $\alpha_M\beta_2$ suppresses proinflammatory M1 polarization in macrophages**

(A and B) Flow cytometry of peritoneal macrophages that were either untreated or stimulated with LPS (1μg/ml) (A) or IL-4 (50 ng/ml) (B) for 24 h at 37°C and subsequently double-stained with anti-F4/80-PE Ab and anti-iNOS (A) or anti-CD206 Abs (B). The data show expression of these markers in the F4/80-positive population, which was > 90 % of total cell numbers. (A: *P<0.05, **P<0.01; B: *P<0.05, **P<0.01 $\alpha_M^{-/-}/ApoE^{-/-}$ *vs ApoE* $^{-/-}$ mice, n=6). The results are representative of three independent experiments. (C and D) Western blot analysis of macrophage lysates from (A) and (B) probed with antibodies to iNOS (C) and CD206 (D) and to β-actin as loading controls. Right panels of C and D show

densitometric analysis of the Western blots with Image J software and the values of iNOS and CD206 band density are expressed as a ratio to β-actin band density. (C: *P<0.01, D: *P<0.05, **P<0.03 $\alpha_M^{-/-}/ApoE^{-/-}$ *vs* $ApoE^{-/-}$ mice, n=6). Images are representative of three independent experiments. (E-F) The levels of IL-6 (E), IL-12 (F) and IL-10 (G) measured in macrophage-conditioned media 48 h post-stimulation with LPS (1μg/ml) (E, F) or IL-4 (50 ng/ml) (G) using ELISA Kits for these interleukins. (E:*P<0.01, F:*P<0.05, **P<0.01, G: *P<0.05, **P<0.001 $\alpha_M^{-/-}/ApoE^{-/-}$ vs $ApoE^{-/-}$ mice, n=6). Three independent experiments were performed.

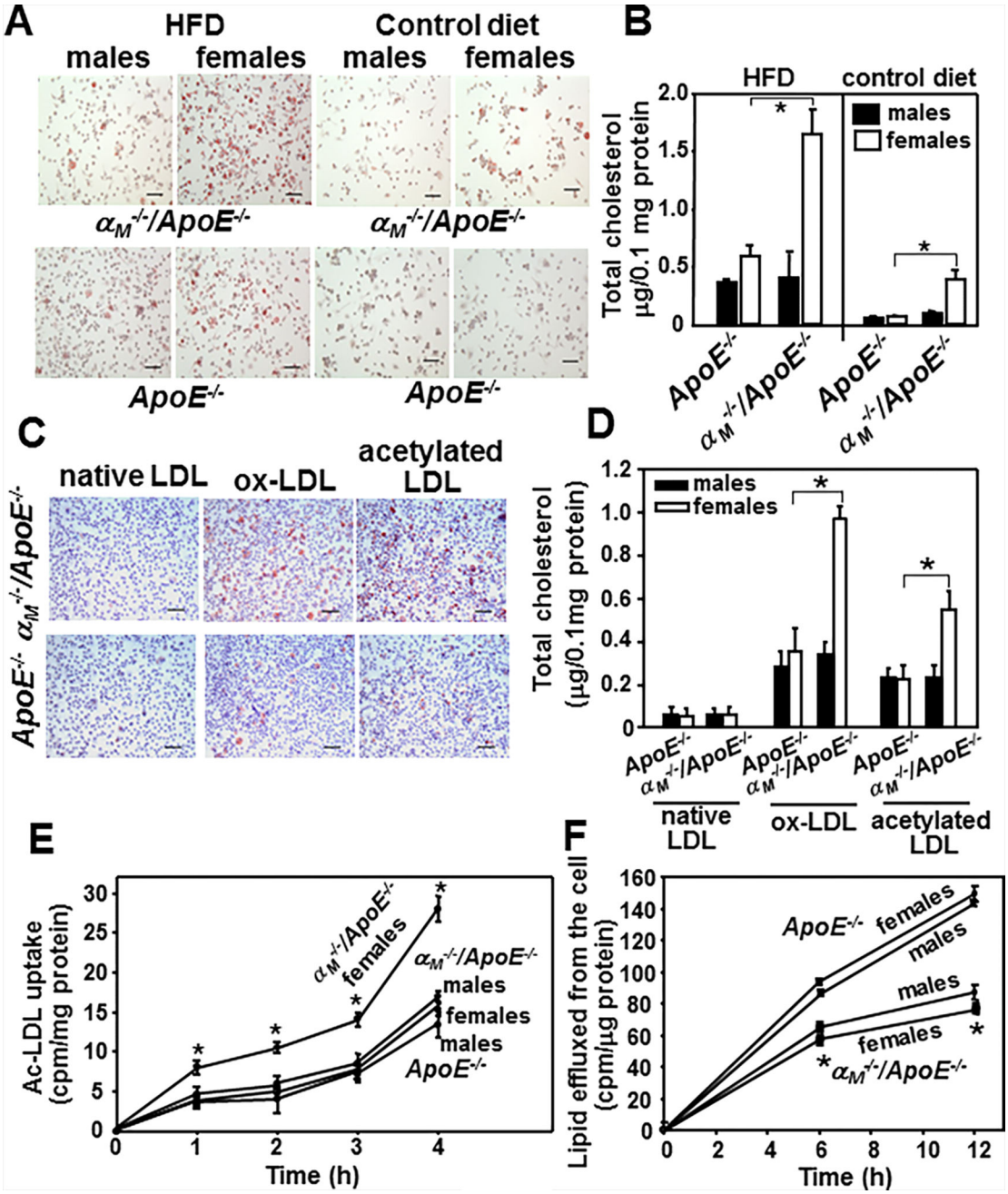


**Figure 4. $\alpha_M\beta_2$ reduces foam cell formation**

(A) Representative images of oil red-O-stained peritoneal macrophages isolated from $\alpha_M^{-/-}$/$ApoE^{-/-}$ and $ApoE^{-/-}$ mice fed HFD or control diet for 16 weeks. Bar size, 32 μm (B) Foam cells were quantified within the peritoneal macrophages population from mouse groups shown in A using Cholesterol/Cholesteryl Quantification kit upon lipid extraction as described in Methods (*P<0.01, female $\alpha_M^{-/-}/ApoE^{-/-}$ *vs* female $ApoE^{-/-}$ mice, n=8). Data are representative three independent experiments. (C and D) *Ex vivo* foam cell formation from peritoneal macrophages of female $\alpha_M^{-/-}/ApoE^{-/-}$ and $ApoE^{-/-}$ mice fed control diet for 16 weeks. Foam cell formation was examined in the presence of native, oxidized or

acetylated LDL for 3 days in culture. (C) Representative images of oil red-O-stained cells. Bar size, 32 μm (D) Quantification of foam cell formation performed as in B (*P<0.001 female $\alpha_M^{-/-}/ApoE^{-/-}$ *vs* female $ApoE^{-/-}$ mice, n=8). Results are representative of three independent experiments. (E) Uptake of acetylated-LDL and (F) Efflux of $^3$H-cholesterol from $\alpha_M^{-/-}/ApoE^{-/-}$ and $ApoE^{-/-}$ peritoneal macrophages was performed as described in Methods. (uptake of acetylated-LDL: *P<0.05 female $\alpha_M^{-/-}/ApoE^{-/-}$ *vs* female $ApoE^{-/-}$ mice, n=6; efflux of $^3$H-cholesterol: *P<0.01 female $\alpha_M^{-/-}/ApoE^{-/-}$ *vs* female $ApoE^{-/-}$ mice, n=6). Data are representative of three independent experiments.

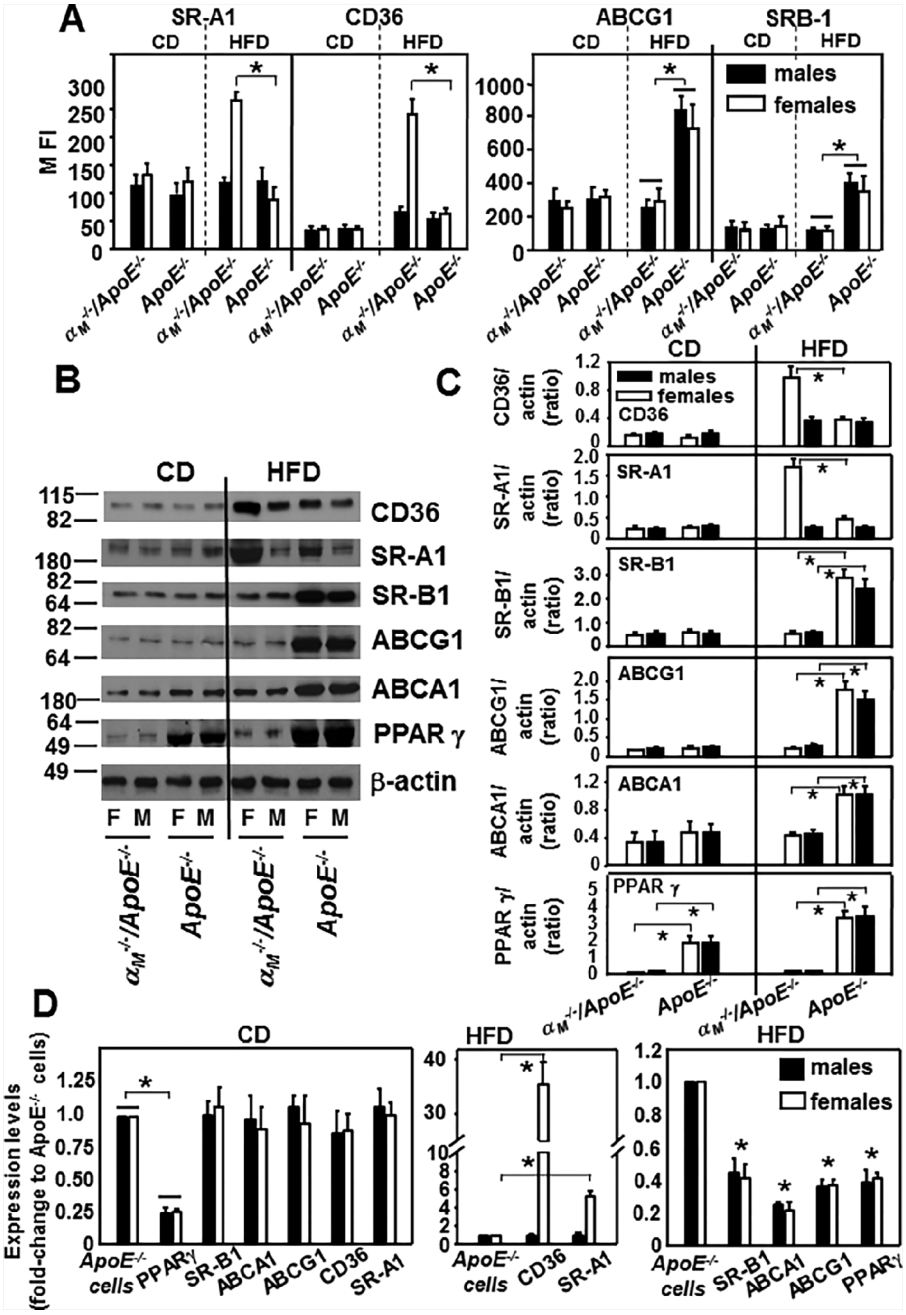


**Figure 5. $\alpha_M\beta_2$ reduces expression of lipid uptake proteins in gender-dependent manner and enhances expression of lipid efflux proteins**

(A) FACS analysis of peritoneal macrophages harvested from $\alpha_M^{-/-}/ApoE^{-/-}$ and $ApoE^{-/-}$ mice fed CD or HFD for 16 weeks. The cells were double-stained with Alexa 488-labeled Abs to the lipid regulating proteins as indicated and with PE-labeled macrophage F4/80 Ab. The data show expression of each lipid regulator in the F4/80-positive population, which was > 80 % of total cell numbers. (left panel: *P<0.01 female $\alpha_M^{-/-}/ApoE^{-/-}$ *vs* female $ApoE^{-/-}$ mice and right panel:*P<0.05 $\alpha_M^{-/-}/ApoE^{-/-}$ *vs* $ApoE^{-/-}$ mice, n=8). The results are representative of three independent experiments. (B) Western blot analysis of macrophage lysates from (A) probed with antibodies to the indicated lipid regulators and to

β-actin as loading controls. Equal volumes of each macrophage lysate from 4 mice of each group were combined, protein assays were performed by Bradford method and equal protein amounts were loaded onto the gel. Images are representative of four independent experiments. (C) Densitometric analysis of Western blots from B. (CD36, SR-A1:*P<0.05 female $\alpha_M^{-/-}/ApoE^{-/-}$ *vs* female $ApoE^{-/-}$ mice; SR-B1, ABCG1: *P<0.01; ABCA1:*P<0.05; PPARγ:*P<0.001 $\alpha_M^{-/-}/ApoE^{-/-}$ *vs* $ApoE^{-/-}$ mice, n=6) (D) Quantitative RT-PCR of transcripts of various lipid regulators in peritoneal macrophages isolated from $\alpha_M^{-/-}/ApoE^{-/-}$ and $ApoE^{-/-}$ mice fed HFD for 16 weeks. Expression levels are plotted as fold change relative to the levels in $ApoE^{-/-}$ macrophages (assigned value=1) isolated from gender matched controls. GAPDH was used as internal control for normalization. (left panel: *P<0.001$\alpha_M^{-/-}/ApoE^{-/-}$ *vs* $ApoE^{-/-}$ mice; middle panel:*P<0.001 female $\alpha_M^{-/-}/ApoE^{-/-}$ *vs* female $ApoE^{-/-}$ mice; right panel:*P<0.001 $\alpha_M^{-/-}/ApoE^{-/-}$ *vs* $ApoE^{-/-}$ mice, n=6).

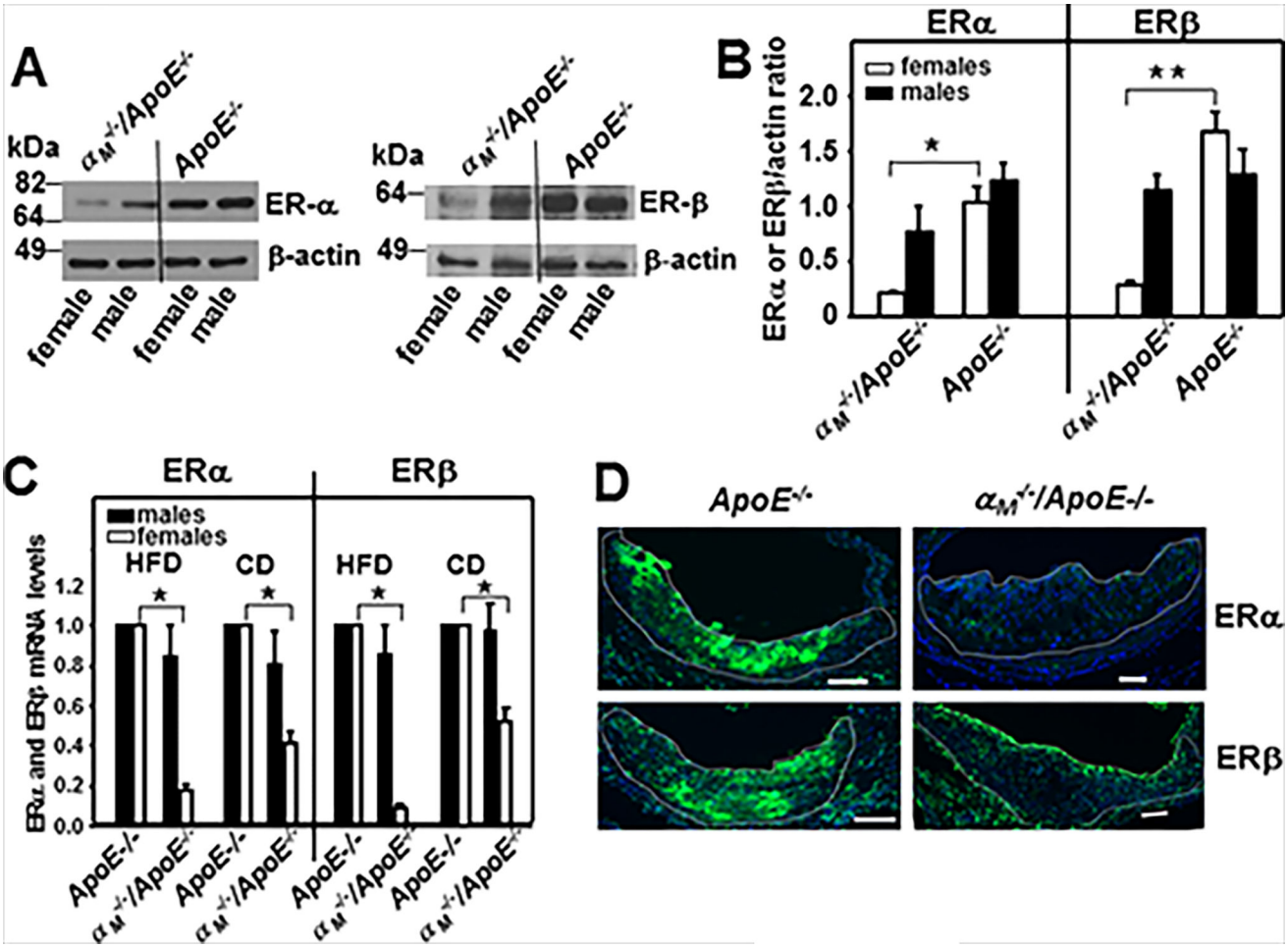


**Figure 6. Macrophages derived from female $\alpha_M^{-/-}/ApoE^{-/-}$ mice show extremely low ERα and ERβ expression levels**

(A) Western blot analysis of peritoneal macrophages harvested from $\alpha_M^{-/-}/ApoE^{-/-}$ and $ApoE^{-/-}$ mice fed HFD for 16 weeks probed with anti-ERα (left panel), anti-ERβ (right panel) or anti-β-actin antibodies. Images are representative of three independent experiments. (B) Densitometric quantification of Western blots described in A. (*P<0.05, **P<0.01 female $\alpha_M^{-/-}/ApoE^{-/-}$ vs female $ApoE^{-/-}$, n=6) (C) Quantitative RT-PCR of transcripts of ERα and ERβ in peritoneal macrophages derived from $\alpha_M^{-/-}/ApoE^{-/-}$ and $ApoE^{-/-}$ mice. Expression levels are plotted as fold change relative to the levels in $ApoE^{-/-}$ macrophages (assigned value=1) isolated from gender matched controls. GAPDH was used as internal control for normalization. (*P<0.05 female $\alpha_M^{-/-}/ApoE^{-/-}$ *vs* female $ApoE^{-/-}$ mice, n=6). (D) Representative images of the aortic root sections stained with anti-ERα (upper panel) or anti-ERβ (lower panel) Abs (green) derived from female $\alpha_M^{-/-}/ApoE^{-/-}$ and $ApoE^{-/-}$ mice on HFD. White lines indicate the boarders of atherosclerotic lesions. Bar size, 64 μm.

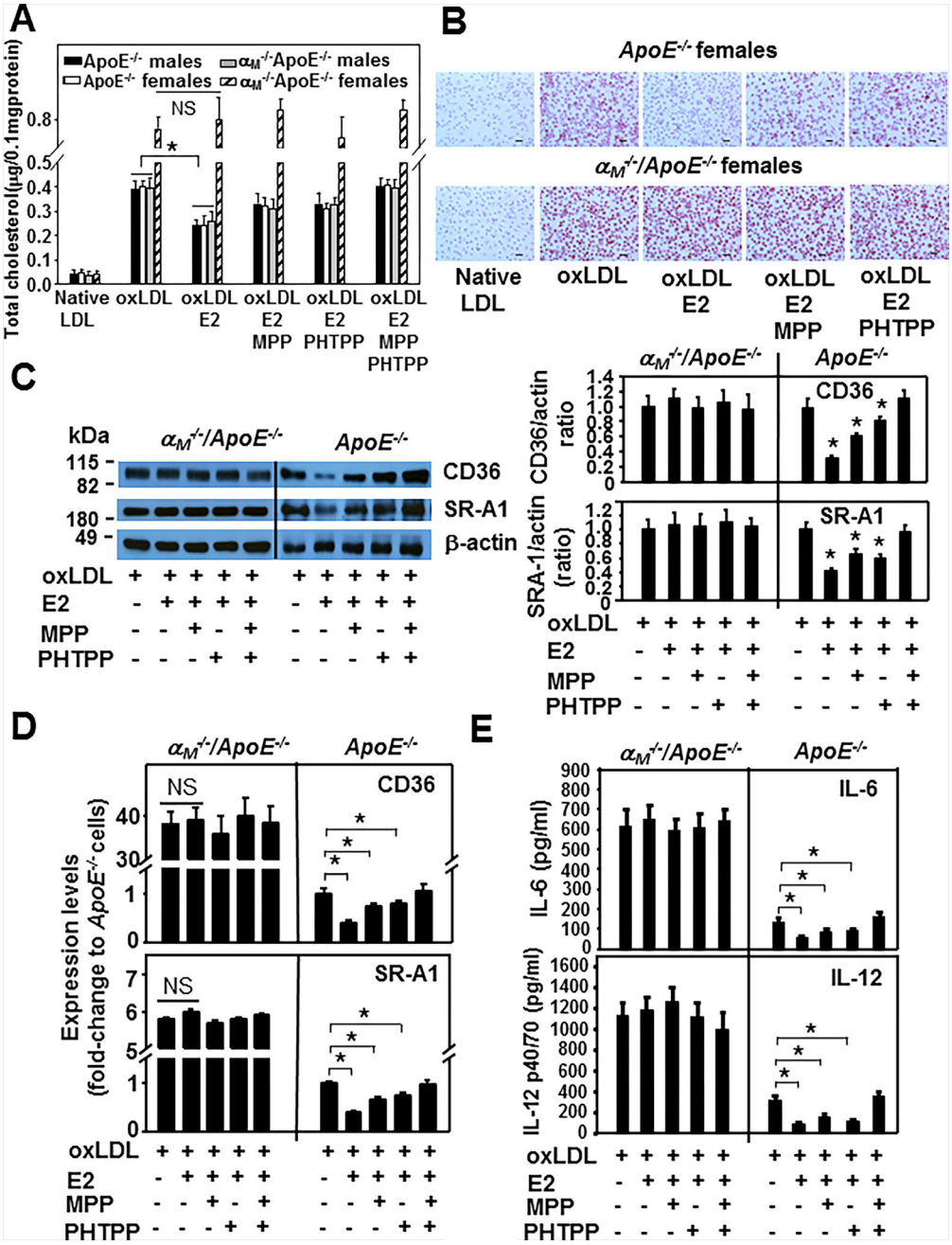


**Figure 7. The effect of $E_2$ on ox-LDL uptake by $\alpha_M^{-/-}/ApoE^{-/-}$ and $ApoE^{-/-}$ macrophages**

(A) *Ex vivo* foam cell formation from peritoneal macrophages of $\alpha_M^{-/-}/ApoE^{-/-}$ and $ApoE^{-/-}$ mice was examined in the presence of native or ox-LDL. As indicated, some macrophages were pretreated with MPP (200 nM), PHTPP (200 nM) or both for 1h and then treated with $E_2$ (100 nM) and ox-LDL for 2 days in culture (*P<0.05 $E_2$-treated *vs* untreated cells, NS, statistically nonsignificant, n=6). Results are representative of three independent experiments. (B) Representative images of oil red-O-stained cells from experiments described in (A). Bar size, 32 μm. (C) (left panel) Western blot analysis of macrophages from female $\alpha_M^{-/-}/ApoE^{-/-}$ and $ApoE^{-/-}$ mice treated as described in (A) probed with

antibodies to CD36, SR-A1 and to β-actin as loading controls. (right panel) Densitometric quantification of the Western blots from left panel. The values are expressed as ratios of CD36 or SR-A1 band densities to respective β-actin band densities. (*P<0.05, $E_2$-treated or $E_2$ ± MPP or PHTPP- treated *vs* untreated cells, n=6). Images are representative of three independent experiments. (D) Quantitative RT-PCR of transcripts of CD36 and SR-A1 in peritoneal macrophages derived from female $\alpha_M^{-/-}/ApoE^{-/-}$ and $ApoE^{-/-}$ mice. The cells were treated as in (A). Expression levels are plotted as fold change relative to the levels in $ApoE^{-/-}$ macrophages (assigned value=1). GAPDH was used as internal control for normalization. (*P<0.001 $E_2$-treated *vs* untreated cells, NS, statistically nonsignificant, P>0.05, n=8). Data are representative of three independent experiments. (E) IL-6 and IL-12 levels in conditioned media collected from equal numbers of adherent female $\alpha_M^{-/-}/ApoE^{-/-}$ and $ApoE^{-/-}$ macrophages, that were treated as described in A. The interleukins were measured using commercially available ELISA kits. (*P<0.05, $E_2$-treated or $E_2$ ± MPP or PHTPP- treated *vs* untreated cells, n=6). Three independent experiments were performed.

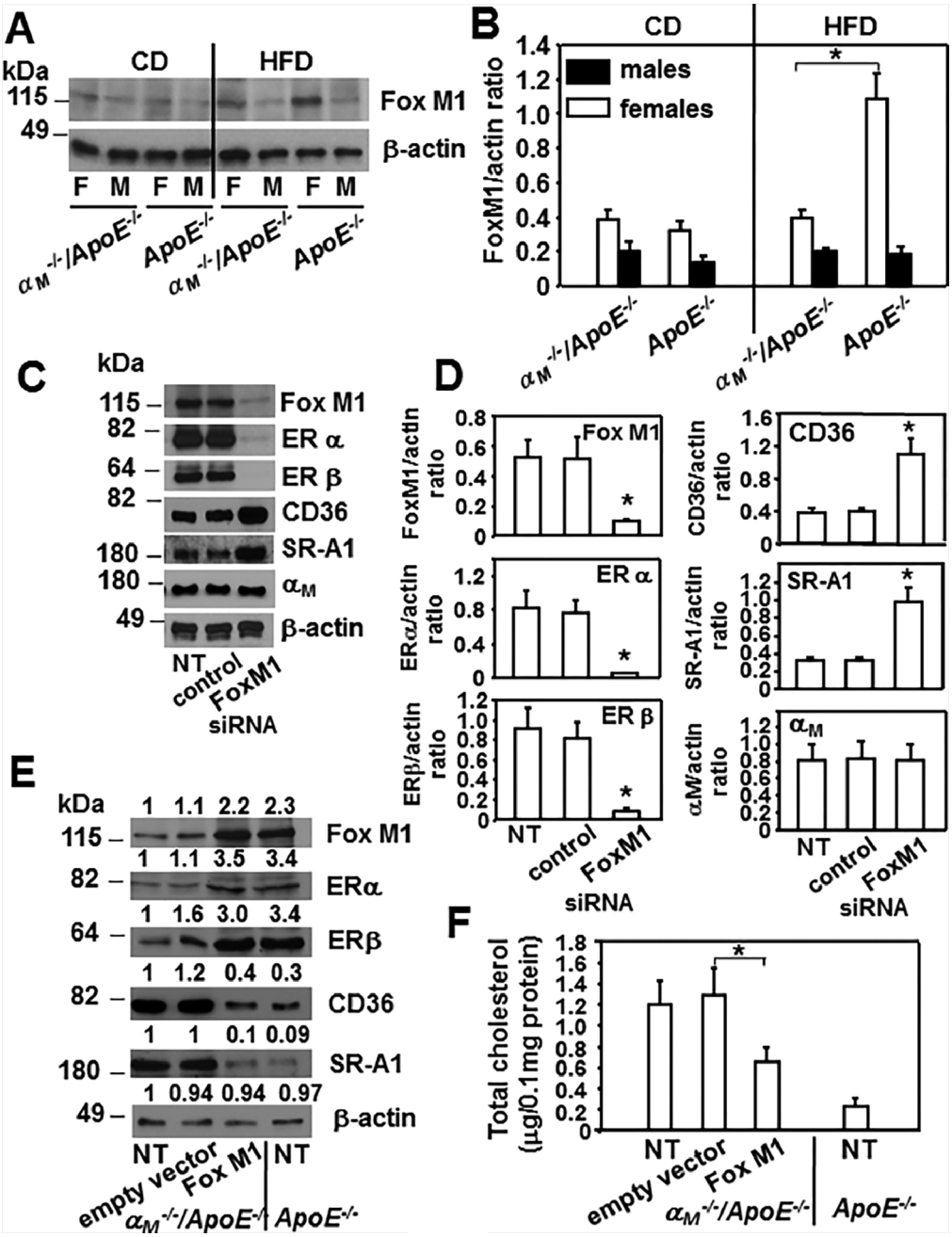


**Figure 8. Fox M1 regulates expression of ERs in macrophages and it is reduced exclusively in female $\alpha_M^{-/-}$/ApoE$^{-/-}$ macrophages**

(A) Western blot analysis of peritoneal macrophages derived from $\alpha_M^{-/-}$/ApoE$^{-/-}$ and ApoE$^{-/-}$ mice fed CD or HFD probed with Ab to FoxM1 and β-actin. Images are representative of 3 independent experiments (B) Densitometric quantification of Western blots from A. (*P<0.05, female $\alpha_M^{-/-}$/ApoE$^{-/-}$ *vs* female ApoE$^{-/-}$ mice, n=6). (C) Western blot analysis of macrophages derived from female ApoE$^{-/-}$ mice that were untreated or treated with FoxM1 siRNA or control siRNA. Western blots were probed with indicated Abs and β-actin as loading control. (D) Densitometric quantification of Western blots from C. (*P<0.05, *FoxM1* siRNA treated macrophages vs untreated or control-siRNA treated cells, n=6). Three

independent experiments were performed. (E) Western blot analysis of female $\alpha_M^{-/-}/ApoE^{-/-}$ macrophages that were untreated or transfected with FoxM1 pcDNA3.1 or empty vector pcDNA3.1 as described in Materials and Methods. Also lysates of untreated female $ApoE^{-/-}$ macrophages were included as control. Western blots were probed with indicated antibodies and anti-β-actin for loading control. Densitometric quantification and values of band densities are shown above each blot and they are calculated relative to the control sample of untreated $\alpha_M^{-/-}/ApoE^{-/-}$, which has been assigned value 1. (F) Foam cell formation was measured as described in Materials and Methods in macrophages treated as in E. (*P<0.05, FoxM1 transfected $\alpha_M^{-/-}/ApoE^{-/-}$ macrophages *vs* transfected with empty vector, n=8). Three independent experiments were performed.

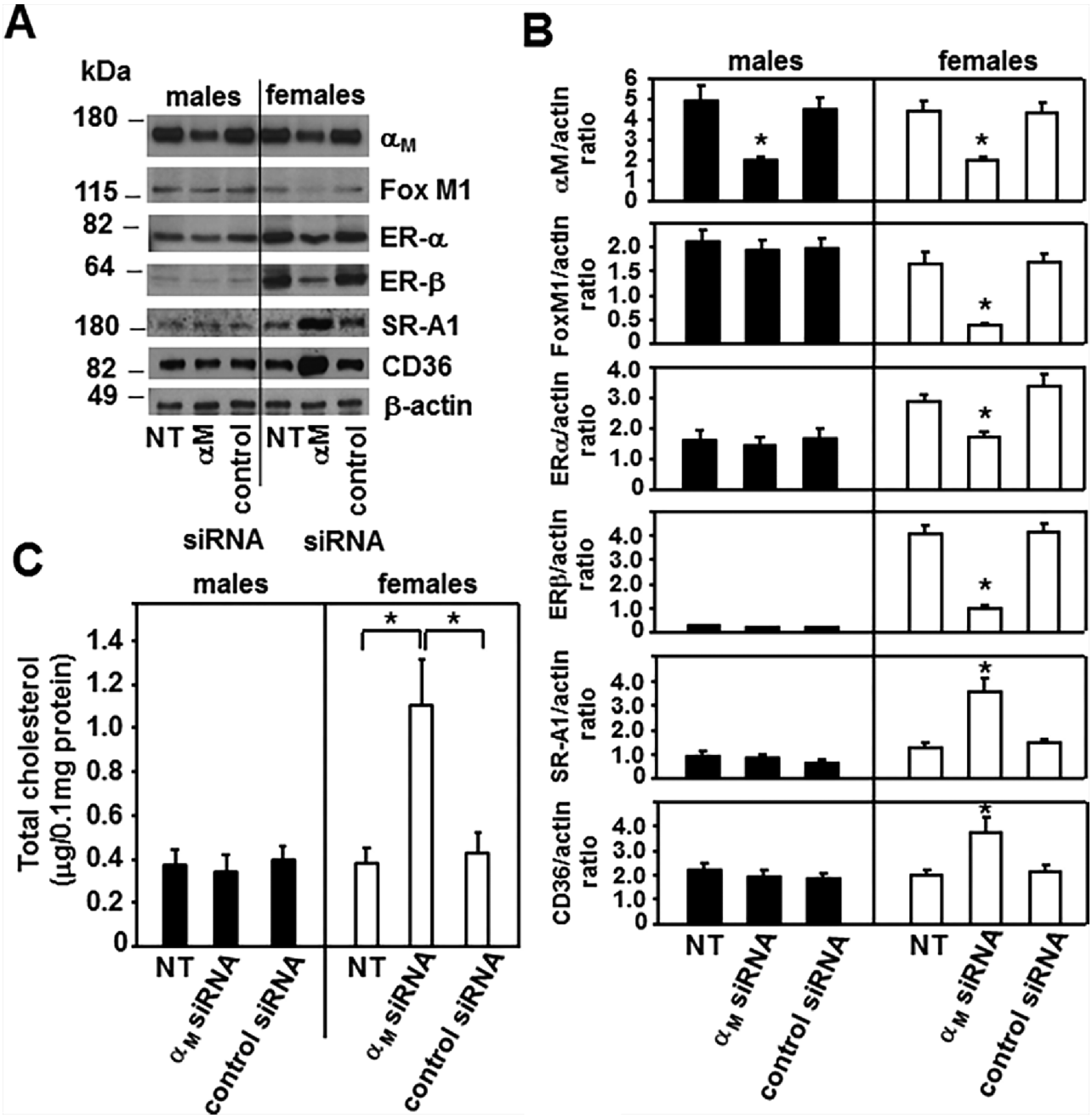


**Figure 9. Reduction of $\alpha_M$ expression in *ApoE*$^{-/-}$ macrophages inhibits ER expression and enhances foam cell formation in a gender-dependent manner**

(A) Western blot analysis of peritoneal macrophages derived from *ApoE*$^{-/-}$ male and female mice were untreated or treated with control or $\alpha_M$ *(Itgam)* siRNA as described in Materials and Methods. The Western blots were developed with respective Abs as indicated and images are representative of 3 independent experiments. (B) Densitometric analysis of Western blots from A. (*P< 0.05 $\alpha_M$ siRNA-treated *vs* untreated or control siRNA-treated *ApoE*$^{-/-}$ macrophages, n=6). (C) Foam cell formation from *ApoE*$^{-/-}$ macrophages that were untreated or treated with control or $\alpha_M$ siRNA was measured as described in Materials and

Methods. (*P<0.05 $\alpha_M$ siRNA-treated *vs* untreated or control siRNA-treated *ApoE*$^{-/-}$ macrophages, n=6). Data are representative of three independent experiments.